University of South Bohemia in České Budějovice

Faculty of Science

Visualization of surface antigens by correlative microscopy

Master thesis

Ayya Tashlieva

Supervisor: Ing. Jana Nebesářová, CSc.

České Budějovice 2017

Master thesis

Tashlieva A., 2017: Visualization of surface antigens by correlative microscopy. M.Sc. thesis in English – 65 p., Faculty of Science, University of South Bohemia in České Budějovice.

Annotation:

Currently Correlative Light- and Electron Microscopy (CLEM) is widely used for high-resolution analysis by electron microscopy (EM) after imaging by fluorescence markers by light microscopy (LM).

The differences in sample preparation protocols for LM and EM create certain difficulties to precise correlation of FLM and TEM imaging. Fluorescent marker GFP that used in present work allows the study of cellular processes and detect ROI, while TEM is used for *B.burgdorferi* ultrastructure study.

The high-pressure freezing (HPF) procedure, freeze substitution (FS) protocol and the correct choice of resin compound for embedding strongly affects the fluorescence preservation. Therefore, acrylic resins with different water content were investigated as a comprehensible variant for cryofixed biological samples for CLEM technique.

Prohlašuji, že svoji diplomovou práci jsem vypracovala samostatně pouze s použitím pramenů a literatury uvedených v seznamu citované literatury.

Prohlašuji, že v souladu s § 47b zákona č. 111/1998 Sb. v platném znění souhlasím se zveřejněním své diplomové práce, a to v nezkrácené podobě elektronickou cestou ve veřejně přístupné části databáze STAG provozované Jihočeskou univerzitou v Českých Budějovicích na jejích internetových stránkách, a to se zachováním mého autorského práva k odevzdanému textu této kvalifikační práce.

Souhlasím dále s tím, aby toutéž elektronickou cestou byly v souladu s uvedeným ustanovením zákona č. 111/1998 Sb. zveřejněny posudky školitele a oponentů práce i záznam o průběhu a výsledku obhajoby kvalifikační práce. Rovněž souhlasím s porovnáním textu mé kvalifikační práce s databází kvalifikačních prací Theses.cz provozovanou Národním registrem vysokoškolských kvalifikačních prací a systémem na odhalování plagiátů.

V Českých Budějovicích, 12.12.2017

Ayya Tashlieva

Acknowledgement

Foremost, I would like to express my sincere gratitude to my supervisor and thesis mentor Ing. Jana Nebesářová, CSc. for scientific guidance, support and help that provided me to choose the right direction.

In addition, I would like to thank RNDr. Marie Vancová, PhD for valuable remarks and suggestions in general.

I share the credit of my work with Mgr. Martin Strnad for important advices during the work.

This thesis would not have been possible unless technicians of Laboratory of Electron Microscopy, Biology Centre of CAS, institution supported by the MEYS CR (LM2015062 Czech-BioImaging) Petra Masařová, Mgr. Martina Tesařová, Jiří Vaněček; Mgr. Tomáš Bílý, Mgr. Jana Kopecká with their valuable advices in a practical plane.

I would also like to express special thanks to Laboratory of Morphology and Rheology of Polymer Materials, Otto Wichterle Centre of Polymer Materials and Technologies, Innovation centre of the Institute of Macromolecular Chemistry, Academy of Sciences of the Czech Republic, namely doc. RNDr. Miroslav Šlouf Ph.D. and RNDr. Sabina Krejčíková, CSc. for help with the experiments and evaluation of the obtained data.

List of used abbreviations

AFS automatic freeze substitution

B. Borrelia

B.burgdorferi Borellia burgdorferi Bb914, a GFP-expressing virulent derivative of strain 297

B.burgdorferi with QDs Borellia burgdorferi with quantum dots

BSA bovine serum albumin

BSK Barbour-Stoenner-Kelly

CCD charge coupled device

CEMOVIS cryo-electron microscopy of vitreous sections

CLEM correlative light- and electron microscopy

EIT indentation modulus

EM electron microscopy

EMS Electron Microscopy Sciences

GLC graphene liquid cell

FLM fluorescence light microscopy

FIB focused ion beam

FS freeze substitution

FWHM full width of half height

GA glutaraldehyde

GFP green fluorescent protein

GMA glycol methacrylate

HIT indentation testing hardness

HPF high pressure freezing

HPMA hydroxypropyl methacrylate

LC lead citrate

LN2 liquid nitrogen

LR London resin

LRW London resin White

NA numerical aperture

NIR near-infrared

PEG polyethylene glycol

QD quantum dot

QDs quantum dots

resp. respectively

ROI region of interest

RT room temperature

RTS rapid transfer system

SECOM scanning electron combined optical microscope

SEM scanning electron microscopy

SIM scanning ion microscopy

TEM transmission electron microscopy

UA uranyl acetate

UV ultraviolet

Table of contents

CHAPTER 1. INTRODUCTION

Single imaging procedure is not enough for additional insight into biological questions, for this reason two or more imaging techniques (e.g. fluorescence- and electron microscopy) are combined to study the one research object or area of interest.[1] CLEM is a universal tool in cell biology at present. At the same time, CLEM is the complicated technique due to different observation characteristics and magnification.

CLEM could disclose the cell surface topology and show structure details of certain region of interest for understanding the complex processes occurring in a cell or tissue. For example, high spatial resolution of TEM gives subcellular details of the area of interest, which was detected before in FLM by fluorochrome in thin optical plane of the thin section. In correlative microscopy and multiply labeling technologies the particulate immunoprobes with different spectral properties are used for increasing sample efficiency and resolution afforded by light and confocal microscopes.[2] "Immunoprobes labeled with fluorescent or particulate markers constitute two of the most powerful reporter systems available for immunocytochemistry"[2].

Technical advances in visualizing antigen – antibody interactions in situ, report systems for the detection of antigen – antibody interactions which provide specificity are available due immunocytochemistry, centered on the distribution of molecules in biological material for obtaining site-specific information.[2]

For better results in correlation, the biological sample usually prepared by the independent methodology because of differences in observation conditions.

Correlative microscopy is quiet successfully applied with cryogenic temperatures. Single particle analysis is available in cryo-EM for macromolecular complexity visualization with helical Fourier inversion methods.[3]

Advancement in the problem of study compatibility in CLEM are currently observed in the SECOM platform (DELMIC B.V., the Netherlands)[4] for integrated fluorescence and electron microscopy and Delphy system (DELMIC B.V., the Netherlands with Phenom-World B.V., the Netherlands)[5] that integrates a tabletop scanning electron microscope with an inverted fluorescence microscope, FEI's CorrSight automated correlative imaging system for correlative workflow (Thermo Fisher Scientific Inc., USA)[6], "MirrorCLEM" system (Hitachi High-Technologies Corporation, Japan and RIKEN, Japan) for FE-SEM SU8200 series (Hitachi High-Technologies Corporation, Japan) where "the field of view (FOV) in a FE-SEM

can move to any region of interest in the LM image and the same FOV can be observed in the FE-SEM"[7], SECOM with FM integrated into SEM chamber by Nanounity (USA)[8].

CHAPTER 2. THE LITERATURE REVIEW

2.1 Basic principles of fluorescence microscopy

Due to high-contrast images (owing to bright properties of the fluorophore molecules, which are easy detectable from background noise) the fluorescence microscopy is a popular instrument in biological studies.

Fluorescence is the physical phenomenon of "absorption and subsequent re-radiation of light by organic and inorganic specimens"[9]. It should be noted that there is also the phenomenon of phosphorescence, a specific type of photoluminescence, but it is usually observes when excitation light is absorbed, but the material does not emit the radiation.

The spatial resolution of fluorescence microscope is not lower than the "diffraction limit of specific specimen features"[9].

Fluorescence microscopy helps to detect and examine the distribution of "spontaneously fluorescent pigments"[10] in "the tissues in translucent and opaque objects"[10], in unstained preparations[10] which cannot be studied "by any other methods"[10]; to serve "translucent objects treated with fluorescent dyestuffs"[11] and useful tool for intravital microscopy[10].

Fluorescence microscopy is based on the principle of illuminating the microscopic object by fluorescent light produced in the object itself.[9] The basic principle of fluorescence microscope, which was presented in 1908 by Köhler A. and Siedentopf H., have a light source (it could be a mercury-vapor lamp or a laser), an excitation filter for specific wavelength isolation and a dichroic mirror for separation of excitation and emission light "in the same light path"[12] (Fig.1).

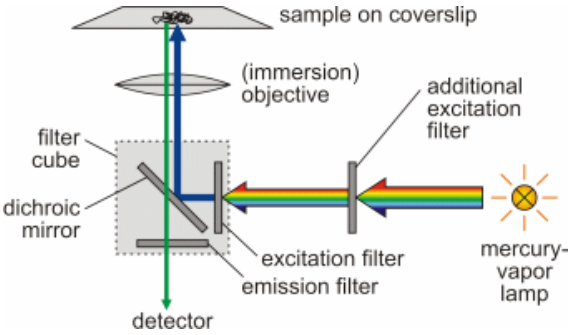

Figure 1. The basic scheme of the fluorescence microscopy principle.[12]

The fluorescence is excited by short wave-length rays "which are focused on the object".[9] The emission light reaches the detector and the fluorescent structures are overlap each other "with high contrast against a very dark background"[9]. To the point, the excitation light $10^5 – 10^6$ times brighter than the emitted fluorescence.[9] The emission filter (Fig.1) blocks the "unwanted excitation wavelength"[9], because the emitted light re-radiates in all directions.[9] The fluorescence microscopy objective is a condenser and light collector contemporaneously.[9] "The full numerical aperture of the objective is available when the microscope is properly configured for Köhler illumination"[9]. The emitted light have longer wavelength that the excitation illumination, that is why it is able to go upward to the detector.[9] The dichroic mirror internal coating absorbs a small amount of excitation light.[9] Emitted fluorescence pass through filter cube before reaching the detector. It helps to get needful wavelength of emission light. Figure 2 shows an integrated "optical block"[9], which consists from an excitation filter, dichromatic mirror and barrier filter.

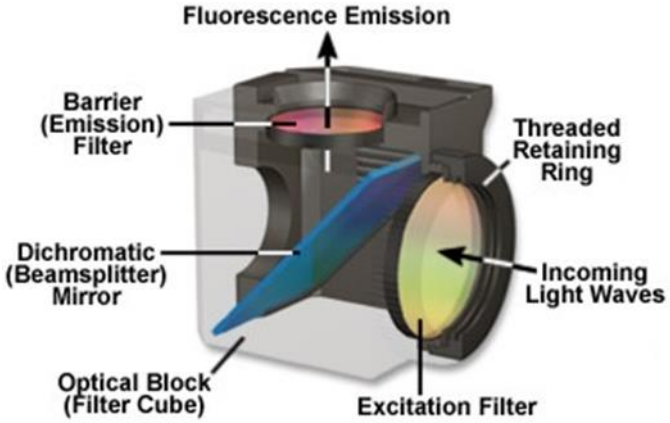

Figure 2. Fluorescence filter cube.[9]

Fluorescence microscope could be adjusted for Köhler illumination due the form of vertical illuminator.[9]

The fluorescent dyes as acriflavin and fluorescin are used in intraviral microscopy, wherein fluorescin allows "simultaneous estimation of the pH of the tissue"[10] of the animal. Should be noted, that due to the problem of correct fixation of a living object, to get the fluorescent image photomicrograph is a bit harder, than for the lifeless one.[10]

Theoretical limit signal/noise ratio (s/n) for fluorescence is proposed by the following expression[13]:

$$s/n = \frac{D\Phi_F\left(\frac{\sigma_p}{A}\right)\left(\frac{P_0}{h\nu}\right)T}{\sqrt{\left(\frac{D\Phi_F\sigma_p P_0 T}{Ah\nu}\right)+C_b P_0 T+N_d T}} \quad (1)$$

Here, Φ_F - fluorescence quantum yield, σ_p - the absorption cross section, T - the constant of time integration of the detector, A - irradiation area, $P_0/h\nu$ - the number of absorbed photons per second, C_b - background count rate value based on the driving power of 1 W, N_d - the dark count rate, D - depending on the instrument accumulation factor.

According to this equation, for increasing the ratio s/n should be used a fluorophore with high quantum yield (Φ_F) and absorption cross section σ_p. The laser beam should be as narrow as far possible. Radiation power P_0 cannot rise uncontrollably as reduces the saturation of the absorption cross section.

2.1.1 FLM in observation of a biological specimen

In biological research applications the fluorescence is the process which “is nearly simultaneous”[9] in virtue of “short time delay between photon absorption and emission”[9].

In cell biology the fluorescence is used to identify the certain proteins[12], the molecules of interest or reaction localization[5]. Fluorescence is characterized with high signal-to-noise ratio, it enables “to distinguish spatial distributions of rare molecules”[9,14]. To observe the particular fluorochrome in cell or tissue it is needed to use in a specimen the molecules, which become visible after illumination.[14] Also exists multiply fluorescence labeling, which allows to “identify several target molecules simultaneously”[9].

For observing the fluorescence emission in cells by fluorescence microscope it is needed to have “appropriate filter packages”[14] due to “the spectral characteristics of the fluorochrome”[14], because with improper filter pack, the fluorochrome may not fluoresce.[14] During localization detecting is needed to be sure that the cell does not glow without fluorochrome, as well as the fluorochrome “is responsible for the localization pattern observed”[14]. It is logical, that mounting material for the object must not to be fluorescent. The presence of fluorescent dye in the biological object is possible to detect by a spectral eyepiece, which helps to recognize the emission bands of the fluorescent light.[10]

By fluorescent microscopy in unstained objects was determined the distribution of fluorescent pigments in animal and plant tissues, such as porphyrins, lyochromes, chrorophyll.

According to the equation (1), high power radiation can destroy the structure of biological objects.[13]

2.2 Fundamental principles of TEM

The main principle of TEM is a transmission of an electron beam through an ultrathin specimen (typically 50-70 nm thick) located on the metal grids. The beam of electrons is focused into thin coherent beam by condenser lens and at the same time is limited by the condenser aperture. The specimen with thickness up to 100 nm is transparent for electrons and transmitted portion of ones is focused by the objective lens. Thus, obtain the image on the phosphor screen/CCD camera and magnified by intermediate and projector lenses (see Fig.3). It's obvious that lighter areas on the image are relate to a large number of electrons passed through the sample. Exterior view of the JEOL JEM-1010 TEM is shown in Figure 4.

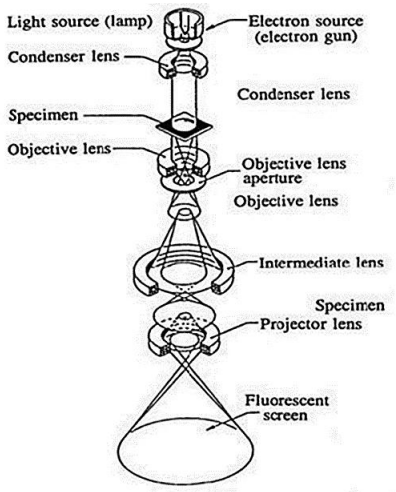

Figure 3. The schematic diagram of TEM [Ref. 15, edited].

Figure 4. JEOL JEM-1010 at Laboratory of Electron Microscopy,[16] Biology Centre of ASCR - Institute of Parasitology. Ceske Budejovice, Czech Republic.

2.2.1 Fixation strategies for TEM in observation of a biological specimen

Morphological study, 3D analysis of cellular interior or immunoelectron microscopy visualization is performed by TEM. Based on the detailed morphologic image TEM helps to recognize the ultrastructures of the biological cells and tissues owing to its near-atomic-level resolution.[17]

Aims of TEM study depend on appropriate preparation technique, wherein should be remembered that the native state sample output in thinner layer leads to higher resolution (but less information is achievable then).[18] TEM produces 2D images, but in comparison with SEM the ones have higher magnification and greater resolution. The chemical fixation or cryofixation as the first stage of preparing biological sample for observing in TEM have the requirement to maintain the size, the shape and 3D internal organization of the sample. There are ample opportunities of TEM studies based on the methodology of sample processing (Fig.5, Fig.6).[19]

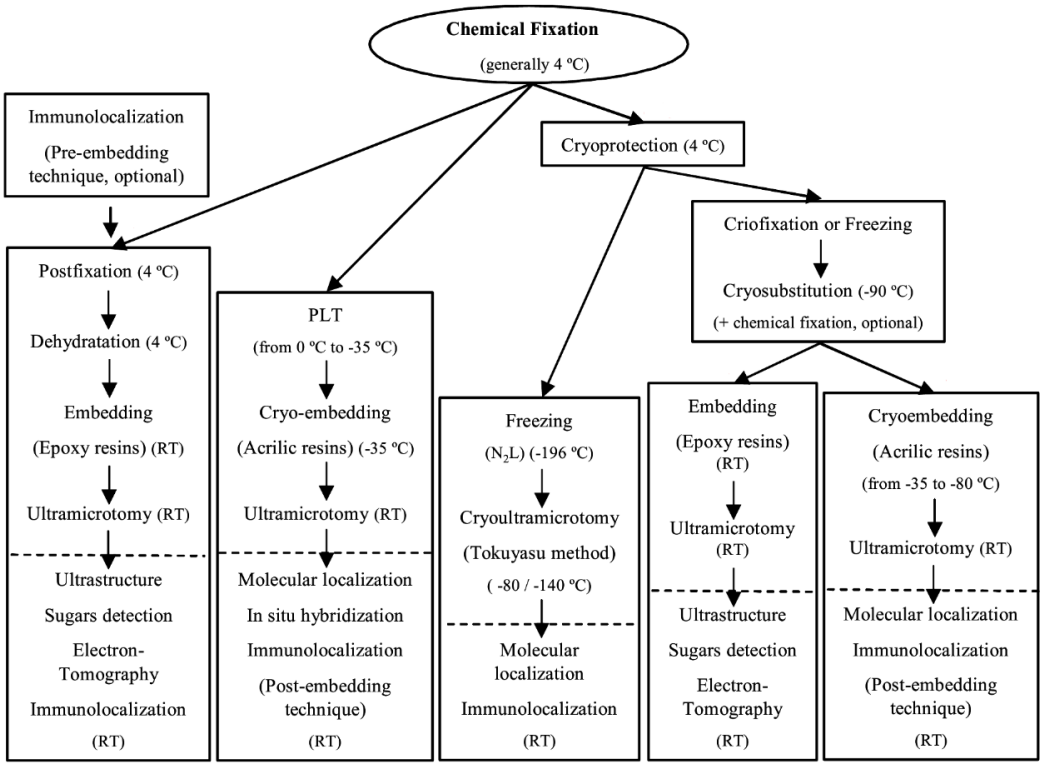

Figure 5. Possibilities of obtaining information from a biological sample prepared by chemical fixation [Ref.19, edited].

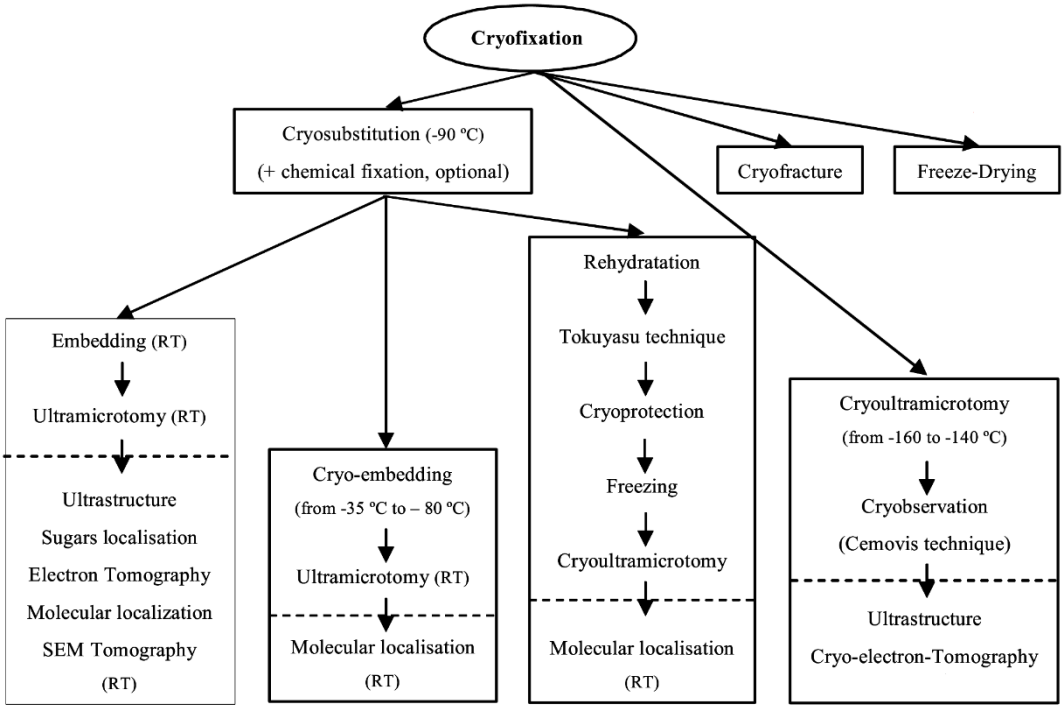

Figure 6. Possibilities of obtaining information from a biological sample prepared by cryofixation [Ref.19, edited].

To get thin section up to 100 nm from the thick biological sample, thinning methods as in CEMOVIS, cryo-FIB or ultracut at RT are used.[20] Whereas cryo-ultramicrotomy requires frozen specimens at ultra-cold temperature to cut the ultrathin sections, ultramictrotomy at RT is used for cutting of samples embedded in polymerized plastic resins.

The biological sample needs to be fixed by chemical agents (glutaraldehyde, paraformaldehyde, acrolein, osmium tetroxide, uranyl acetate, etc.) or cryofixation (progressive lowering of the temperature or high pressure freezing), for obtaining the ultrastructure of the tissues close to the living biological material. To view the biological material in EM is important precondition to dehydrate the biological material by an organic solvent (alchohol, acetone, ethanol, methanol, etc.); it maximally retains the size, shape and internal organization of the sample. For sectioning, the sample is necessary to embed in an epoxy-type resin (Spurr's, Embed 812, Durcupan, etc.) or in an acrylic resin (LRWhite, LRGold, Lowycryl, Unicryl, etc.) [Appx.1]. The additional condition for getting high contrast images by TEM is contrasting of biological samples by heavy metals (osmium tetroxide, lead citrate, uranyl acetate). van Driel L.F. et al. warns for faint contrast in sections because of incompatibility with osmium tetroxide treatment.[21]

Because in HPF technique intracellular gaseous spaces collapses e.g. as in lung tissues, these compartments needed perfluorocarbon to substitute the air in the alveoli.[22]

Although the living specimens cannot be viewed using TEM due to requirement to be a vacuum in the inner space of the microscope, Park J. et al. have declared the possibility of direct observation of wet biological samples by TEM. An influenza viruses were in their native buffer solution, encapsulate by multilayer graphene sheets (GLC).[23]

2.2.1.1 Chemical fixation

Chemical fixation is the most common way of dealing with specimen preservation; it is used for the immobilization of biological processes in cells. Despite the positive result in stabilizing the cellular components in large specimen, there are some drawbacks of this method, as killing the cell content by fixative.

Fixative solutions for LM and EM composed of fixative agent (coagulant or non-coagulant) and vehicle [Appx.2].[24]

For TEM studies, due to slow penetration rate of glutaraldehyde and OsO_4, the tissue block should not exceed 1 mm^3 and the time of fixation is 4 h fixation at RT or overnight at 4 °C (immunological or enzymatic studies). TEM samples "should be fixed using a slightly hypertonic fixative"[24], while SEM specimen usually fixed under or near isotonic condition.

2.2.1.2 Physical fixation

Cryofixation and microvave fixation are physical methods of fixation. Such techniques allow stopping active cellular process in a split second, what is impossible in chemical fixation due to slow penetration rate of fixing agents. Microwave irradiation is able speeding up chemical reaction during chemical fixation, that shortens the processing time, but generated heat may damage the biological sample components.

2.2.1.2.1 Cryofixation

This physical fixation is used to achieve ultrastructural and biological preservation.

Cryofixation stops the cell motion and metabolic activity outright by vitrifying cell water. Rapid freezing of the sample to the temperature of liquid nitrogen (−196 °C) or below prevents ice formation. This technique is very often used in the combination with freeze

substitution method (FS), which provides the best morphological preservation of biological samples for EM. There are many methods (plunge, spray, propane-jet and high pressure freezing (HPF)), which are used for the vitrification of biological samples. HPF is capable to vitrify the specimen layer up to 200 μm in thickness. HPF preserves the specimen in the native size and shape avoiding internal damages by ice crystal formation, because the volume of ice impeded by external high pressure which suppresses ice crystal formation (Le Chatelier's principle)[18]. Inter alia vitreous water could be cut.

2.3 Specimen transfer from FLM to TEM without loss of ROI

The mutually exclusive requirements prevent simultaneous use of CLEM in study of biological specimens. The main factor is that samples for TEM must be dehydrated, whereas in FLM the ones are typically persisted in a hydrated state. The other factor is that the fluorescence signal can be destroyed by high voltage electron beam in TEM.

Photobleaching or fading is an universal problem in CLEM procedure, which results in underestimating and poor imaging of the labeled structures or in the worst case, in no detection at all. To observe in prolonged period, the mounting media could be supplemented with ascorbic acid.[25]

Correlating ROI by CLEM without visible in FLM and TEM landmarks sometimes is impossible. Although the electron imaging destroys the fluorescence signal, reverse back to fluorescence imaging following electron microscopy is almost impossible. The possibility of re-examining samples with either microscopy technique would give "considerable advantages over traditional methods"[26]. Combination of SIM and FLM for obtaining topographical and biochemical information at nanoscale resolution without destroying the fluorescence signal was reported by Bertazzo S. et al. in 2012.[26] By their investigation, SIM uses a gallium beam (which can be used with fluorescent probes without loss of fluorescence[27, 28]) to extract secondary electrons from a surface and yet generates an electron micrograph.

The universal coordinate system for ROI retrieving in CLEM could be defined by using specially designated index grids for TEM.

2.3.1 Fluorescent nanocrystals vs. organic fluorophores

Fluorescent nanocrystals (also known as QDs) are the source for engineering of stable and "bioadaptable"[29] fluorophores due to their "surface functionalization"[29]. Nanocrystals are

stable against photobleaching, have narrow, symmetric emission spectra, that prevent crosstalk in multicolor labeling,[29] that is why they are preferable to organic fluorophores.[29]

Carbodiimides, glutaraldehyde are bifunctional cross-linking reagents which are able to incorporate the fluorescent label into a biopolymer.[29] This helps to have better control of fluorescent label linking place (the center mark). To increase the signal it is necessary to have fluorophores with high quantum yield, large absorption cross section and high photostability. The substances belonging to the class of rhodamines, cyanines and oxazines are often used as the labels of organic compounds.[29]

The QDs, which are most frequently used today, are made up of nanocrystals CdSe-core coated with ZNS-shell, since the ones determined by their high brightness and high chemical- and photostability.[29] By varying the size of the QDs core, it is possible "to customize" the nanocrystals to emit fluorescence by any fixed optical range.

It is important, that QDs of any color absorbs light in a broad spectrum, including UV, and then converting it into fluorescence strictly with predetermined wavelength.[30] The spectral emission line of QDs is symmetrical, it's width at half-maximum (FWHM) is usually 25-30 nm.[31] The ability to initiate QDs with various diameters (different colors of fluorescence light), but with one wavelength provides an unique opportunity for multiplexing.

Next is observed phenomenon of QDs blinking. It occurs due the fact, that electrons or holes are periodically held in surface defects in the crystal structure of reserve transcriptase, which prevents their emitting recombination and thus fluorescence QDs emission. QDs surface passivation or QDs in the implementation of the polymeric matrix gives possibility to substantially reduce the effect of blinking. This makes the QDs radiation source unit with a molecular size (2-10 nm).[32]

The fluorescent proteins are used for visualization of proteins in live and fixed cells by FLM. Usually in polymer embedding protocol the fluorescent proteins are quenched by "the acidic, dehydrated and oxidizing conditions"[33].

Organic dyes have long tail in their emission spectra, which extends far into the red area – it causes imposition of signals from different fluorophores. That is why this disadvantage limits the number (up to 4) of color labels for multiplexing detection.[29] The detection system for organic dyes is complicated due to the necessity to have a light source for each dye, because of their excitation differences.

In optical electron microscopy so-called “green fluorescent protein” (GFP) finds use as an alternative to traditional fluorophores . It was originally isolated from some marine organisms and got its name from the ability to produce fluorescence in the green part of spectrum. The source of protein – a polypeptide of 238 amino acid residues, derived from the jellyfish Aequorea Victoria, it absorbs radiation in the UV and blue spectral range and emits in the green.[34] GFP will not move anywhere after targeting to intracellular location.[35]

Protein tags can be incorporated into the protein by genetic engineering. For this process the part of the DNA coding for the protein is injected with plasmid DNA code by GFP. Thereafter, the protein synthesized in a living cell will contain a portion, providing a high level of fluorescence. [36, 37]

All known fluorophores, used for LM have photobleaching property, to increase the duration of observation antifade mountants were designed. The mountants could be aqueous (for example, FluorSave™ Reagent[38] by Merck Millipore, a part of Merck, USA), glycerol-based (for example, ProLong® Gold Antifade Mountant[39] by Thermo Fisher Scientific, USA) and plastic based (for example, Permount Mounting Medium[40] by EMS, USA).

2.4 CLEM as a combination of FLM and EM techniques

Different fluorescent markers are used to visualize cellular components, protein distribution, biochemical reaction in living cells in FLM. The resolution is limited in such observation due to diffraction, unlabeled structures in the vicinity. Frequently, the labeled structure details remain obscure too. The super-resolution microscopes have shifted the diffraction barrier to 20-60 nm[41], but the reference space still could stay invisible.

EM helps to achieve higher resolution imaging. Moreover, it “reveals organelles, membranes, macromolecules, and thus aids in the understanding of cellular complexity and localization of molecules of interest in relation to other structures”[42].

Combination of fluorescence and EM techniques with different resolution limits[43, 44] is difficult to get, but recently high resolution technologies give chance for fluorescent probes, which are capable of generating contrast for electron microscopy. Correlative microscopy allows “a particular cell to be studied from the micron to the nanometer scale while maintaining spatial orientation”[42].

Correlative imaging helps to gain additional morphological information of the biological sample, to compare the obtained information with the other methods.[43, 45, 46]

Because in CLEM technology are used two separate microscopes, it is possible to use super resolution fluorescent microscopy too.[33, 47]

CLEM - the combination of the labeling power of fluorescence imaging and the high-resolution structural information of electron microscopy – is the perfect tool to study the complex relation between form and function in biology.

CHAPTER 3. METHODS

HPF procedure, FS protocol and the correct choice of resin compound for embedding strongly affects the fluorescence preservation in a biological sample. Therefore, acrylic resins with different water content were investigated as a comprehensible variant for cryo-fixed virulent *B.burgdorferi* Bb914, a GFP-expressing virulent derivative of strain 297 in CLEM technique.

3.1 Object of study

3.1.1 Bacterial strains and culture conditions

Virulent *B.burgdorferi* Bb914, a GFP-expressing virulent derivative of strain 297 (5 ml of isolate in glycerol stock solution) were cultivated in Barbour-Stoenner-Kelly-II (BSK-II) medium without gelatin (50 ml in a sealed sterile culture tube for gas balance) containing 6% rabbit-serum (Sigma-Aldrich Co. LLC.) to late logarithmic phase (1×10^8 spirochetes per ml) for 7 days at 34°C.

The number of the spirochetes per milliliter of media was determined using Petroff-Hausser counting chamber with low-power magnification and dark-field illumination and found to be up to 1×10^8 spirochetes per ml.

50 ml of cultivated *B.burgdorferi* was devided into Eppendorf® Safe-Lock microcentrifuge tubes (Sigma-Aldrich Co. LLC.) with 1.5 ml volume and centrifuged with 4000 rpm for 3 min at 15°C to maximize the number of spirochetes in content. The cell pellet was collected in the Eppendorf® Safe-Lock microcentrifuge tube and centrifuged again under the same conditions for 1 min.

Resuspension of 1×10^8 spirochetes per ml was done in 1.5 ml BSK-II medium with adding 20% bovine serum albumin (BSA) and kept at 24 °C until HPF procedure was done. The buffer solution had pH=7,2.[50]

3.1.2. Embedding media

3.1.2.1. Water-miscible embedding media

Several acrylate resins were tested for their water miscibility as the assumption that water content could play important role in the fluorescence preservation in those resins.

The water was purified by GORO AQUA 65 (GORO, spol. s r.o., Czech Republic) reverse osmosis system with output of 10 l/h.

The mixing processes must be done in a well-ventilated fume hood, to avoid dermatological problems the use of gloves is needed.

3.1.2.1.1 Hydroxypropyl Methacrylate

The HPMA resins of different water content were prepared by addition of 5%, 10%, 15% of water into the prepolymer.

To prepare a prepolymer, 0.03 g azobis was added into 30 ml of HPMA in a beaker and heated with stirring on the heating plate until steaming. Then rapid cool was done in the ice bath. The goal of the process was to obtain liquid-viscous consistency of the prepolymer. After the series of "heat-rapid cool", the water was added. The recommended condition is to stir the tissue during the infiltration process to achieve "desirable infiltration"[51]. The final polymerization was achieved by long wave UV irradiation by adding 0.25% (by weight) of benzoin ether (0.5% w/v) and by heating to 50°C by adding 0.8% (by weight) of benzoyl peroxide as chemical initiators. Infiltrated tissues were polymerized in polypropylene flat bottom capsules (Ted Pella, Inc., USA) closed with leaving as little air as possible.

The necessary condition for HPMA kit is storage in the darkness.

3.1.2.1.2 Glycol Methacrylate

This resin has low viscosity and penetrates tissue easily, preserving morphology without crosslinking.[52] The manufacturer (EMS, USA) recommends to prepolymerize the solution partially to reduce the swelling of a specimen,[10] but I did not made this step.

The GMA resins of different water content were prepared by addition of 3%, 6%, 9% of water into the low acid monomer with the condition of mixture constant cooling in the ice water bath.

35 ml mixture containing of 97% of GMA and 3% of water was mixed with 14.7 ml of 98% butyl methacrylate with 2% 2,4 dichlorobenzoyl peroxide and 0.3 g 2,4 dichlorobenzoyl peroxide. The final polymerization was achieved by long wave UV

irradiation by adding 0.25% (by weight) of benzoin ether (0.5% w/v) and by heating to 50°C by adding 0.8% (by weight) of benzoyl peroxide as chemical initiators. Infiltrated tissues were polymerized in polypropylene flat bottom capsules closed with leaving as little air as possible.

3.1.2.1.3 Polyethylene Glycol – Glycol Methacrylate mix

30,25 ml of GMA (see 3.1.2.1.2.) was mixed with 0.5 ml of PEG (1% v/v) on the hot-plate with stirring function. For present study 3%, 6% and 9% of water was added to this mixture and 0.25% (by weight) of benzoin ether (0.5% w/v) for polymerization was achieved by long wave UV irradiation and 0.8% (by weight) of benzoyl peroxide for heating to 50°C. Infiltrated tissues were polymerized in polypropylene flat bottom capsules closed with leaving as little air as possible. The manufacturer warns about the possible formation of bubbles inside during polymerization and does not consider it as a problem, in addition section staining by UA and LC is possible.[53]

3.1.2.1.4 Nanoplast

This resin does not need dehydration step by organic solvents during embedding process of the biological sample. At the same time, Nanoplast declared by the manufacturer as media that permits to get excellent structural resolution without section staining, but it is more brittle than epoxy resin.[54]

In present work 10 g of hexamethylol-melamine-methyl ether (70% in water) was mixed with 0.2 g of p-toluene sulfonic acid to get medium hardness of the embedded blocks and 10 g of hexamethylol-melamine-methyl ether (70% in water) was mixed with 0.25 g of p-toluene sulfonic acid to get hard blocks (usage for extremely thin sections). During stirring before dissolving, the solution was on the 65°C heating plate, and then it was left for 1 hour before heat polymerization at 60°C for 5 days. Polymerization process included drying for 48 hours with desiccator in the oven and then left for hardening (new desiccator was given) for the remaining term.

3.1.2.2. Hydrophilic embedding media

3.1.2.2.1 Lowicryl K4M

Lowicryl K4M is highly cross-linked acrylate-based embedding medium with low viscosity at low temperatures (usable up to -35°C).[55]

For preparing by heat polymerization at 60°C the Lowicryl K4M embedding solution is needed to protect against incorporation of oxygen during stirring because of reducing the polymerization quality. 2.7 g of triethylene glycol dimethacrylate was gently mixed with 17.3 g of mequinol and 0.1 g of benzoin methyl ether by glass rod until the initiator completely dissolved inside.

The manufacturer (EMS, USA) recommends to replace benzoin methyl ether on benzoin ethylether (same amount) if polymerization in in the range -50°C to 0°C, 0.3% (by weight) dibenzoyl peroxide if polymerization is thermal (60°C). The hardness of the resulting block can be changed by a different amount of triethylene glycol dimethacrylate (up to 20 g).

The UV polymerization was done by long wavelength UV in polypropylene flat bottom capsules closed with leaving as little air as possible, for 24 hours at -35°C followed by 6 days of natural UV polymerization at -6°C to 2°C at open space.

3.1.2.2.2 LR White

LR White was given by manufacturer (EMS, USA) in a catalyzed form that was needed to kept at 4°C or lower. If the resin became more viscous it is not recommended to use it. For heat polymerization 3.5 g of LR White was mixed with 0.0692 g benzoyl peroxide by magnet stir at 5.6°C for 20 min and given into gelatin capsules for 51°C heat polymerization for 48 hours. For UV irradiation 3.5 g of LR White was mixed with 0.0176 benzoin methylether by magnet stir at 5.6°C for 20 min and given into polypropylene flat bottom capsules for long-wave UV polymerization at -20°C for 24 hours and some resin samples were polymerized at 20°C for 48 hours.

3.1.2.3 EMbed 812

To prepare the embedding mixture for medium hardness of the resin block, 20 ml of EMbed 812, 16 ml of dodenyl succinic anhydride, 8 ml of Methyl-5-Norbornene-2,3-Dicarboxylic anhydride and 0.66 ml of 2,4,6-Tri(dimethylaminomethyl) phenol were mixed together. This process was done with warming up the resin and the anhydride to 60°C, to make them more liquid (convenient for mixing).[56]

This mixture could be stored for up to 6 months at 4°C, but freshly prepared medium was preferred in accordance with manufacturer recommendations.

EMbed 812 was polymerized by 60°C heat during 24 hours in polypropylene flat bottom capsules.

3.2 Sample preparation for CLEM

Among different methodologies, HPF preparation technique followed by fixation in FS device with resin embedding is still experimental work for certain biological systems. The main idea is to preserve fine structure of biological sample much close to its native and physiologically active state with good resolution for EM.

3.2.1 HPF preparation technique

HPF is fast technique and therefore it stabilizes all cellular components simultaneously without minimal ice crystal formation. In present study we were used Leica EM PACT2 (Leica Microsystems, a part of Danaher, Germany) with sample carriers where bacterial suspension were given. This process was important in accuracy, because air pockets or small bubbles inside of placed sample into inner cavity of the specimen holder could result specimen damage or even lost. The suspension of *B.burgdorferi* was centrifuged in 20% BSA diluted in spirochete growing media (BSK-II) and thickened by discarding supernatant. This dense slurry was divided by micropipette into aliquots to brass specimen carriers under the stereo microscope. These carriers had round flat shape with a small pit with small hole in center, the size of used holders were 1.2 mm in diameter with 200 µm depth and 0.5 mm thickness. The carrier with specimen inside was held in the rapid loader for automatically freeze in RTS of Leica EM PACT2. For freezing process the rapid loader with mounted in it the flat specimen carrier loaded onto loading platform. After loading of the flat specimen pod, it was mounted on bayonet loading device by matching bayonet connections and turned counterclockwise to lock bayonet.

The RTS triggers freezing, the process of ejecting by RTS the Rapid Loader and automatic high pressure completion had taken only 2.5 sec. The rapid freeze specimen was ejected into LN_2 bath automatically and carefully collected in container with liquid nitrogen, for the next stage of processing by AFS. Because the pod was used few times, it was completely dried by hairdryer after each use, by manufacturer recommendations.

3.2.2 Fixation and embedding process in FS device

Rapidly frozen biological samples were dehydrated in FS unit. FS device with a gradual temperature change avoids detrimental effects of ambient temperature dehydration on the biological sample ultrastructure. This process removes water and allows the crosslinking of cellular components. Moreover, FS embedding can preserve antigens for immunolabeling.

The organic solvents as acetone, ethanol and methanol were used in different protocols during this study.

The program with shorter time was set up for agitation device with methanol reagent as the next:

Table 1.

Program view for Leica EM AFS2 (Leica Microsystems, a part of Danaher, Germany).

	T_{start} (°C)	T_{end} (°C)	Slope (°C/hod)	Time (hour)
1.	-90	-90	0	03:00
2.	-90	-20	30	02:20
3.	-20	-20	0	01:00
4.	-20	-20	0	01:00
5.	-20	-5	10	01:30
6.	-5	-5	0	13:00
7.	-5	-5	0	48:00

As can be seen from the Tab.1, FS started with very low temperature (i.e., up to -90°C) that prevented formation of secondary ice crystals during rise of temperature in fixation and embedding process. It means recrystallization was absent during the FS run and ultrastructural changes in biological sample were minimal. As the samples warm up (i.e., up to -5°C), the crosslinking activity of the chemical fixatives present in FS medium was activated. In order to prevent the sample damage by temperature, all used solutions (organic solvents, resins), a stainless forceps, a tube for solution drain and plastic pipettes (3 ml BRAND® pipettes (Sigma-Aldrich Co. LLC., USA)) for manipulating were precooled in the processing chamber of Leica EM AFS2. For this purpose, prepared solutions were given in Leica EM AFS2 chamber in advance in the 2 ml Sarstedt tubes. The substitution medium (100% methanol+ 2% GA+5% water) provided in four 5 ml glass bottles were precooled as well before use.

The specimen carriers were transferred in the chamber of Leica EM AFS2. The temperature of the chamber was already customized to -90°C. The sample carriers were warmed to -90°C and sub-solution thawed with release of samples on the bottom of plastic

flasks. The freeze substitution started at -90°C and for 3 hours the spirochetes were left in 100% methanol+2% GA+5% water for the test sample and 100% methanol+2% GA for other ones. The test sample was prepared for GMA low acid resin for comparison with GMA low acid resin embedding result without water content in substitute medium. For fixative uniform distribution through the sample, the process of dissolution was repeated with 30°C/hour slope up to -20°C. Then the spirochetes were left for one hour at -20°C in Leica EM PACT2 specimen carriers in 100% methanol+5% water for the test sample and 100% methanol for other ones. Prepared beforehand resins were diluted in 100% methanol for required concentrations. The 30% of resin in methanol filled the glass bottles with specimen carriers for 1 hour, and then was change for 70% of resin in methanol and during this step the temperature raised up to -5°C. Then the liquid content in the glass bottles replaced by last needed concentration in 100% methanol, which was 91%, 90% and 95% of GMA low acid, HPMA, HPMA resp. and left overnight. Next day the specimen carriers with spirochetes were prepared to move in determined polypropylene flat bottom capsules with 7.92 mm inside diameter by sample release. In 91%, 90% and 95% of GMA low acid, HPMA, HPMA resins resp. were added accelerators, as ether for GMA and 0.5% benzoin methyl ether for HPMA resp. for the final change of resin. The propylene capsules were filled as 1/3 with resin + accelerator, by 3 ml BRAND® pipette the biological sample was transferred on the surface of resin drop inside the propylene capsule and filled up to the brim with opportunity to avoid air bubble when closing the capsule cap. The resin was polymerized by long-wave UV light (over 3150 Å wavelength) for 48 hours inside of Leica EM PACT2 chamber at -5°C.

The second variation was done by Leica EM AFS (Leica Microsystems, a part of Danaher, Germany). 25%, 50%, 75% and 95% of HPMA resin were used for infiltration and with -20°C warming step 95% acetone was given for 30 min as the organic solvent, then it was replaced by 95% ethanol (2 times change for 30 min), followed by resin infiltration: 25% HPMA for 60 min, 50% HPMA for 85 min, 75% HPMA for 100 min and 95% HPMA overnight. UV polymerization was done after 95% HPMA substitution for the same fresh solvent. Four test samples from these resin series were covered by foil, just top and bottom of the propylene capsules were not covered for UV long-wave light.

In third variation, HPMA resin from different manufacturers (Electron Microscopy Sciences, USA and Fluka, BioChemika, Sigma-Aldrich Chemie GmbH, Switzerland) with different water content as 5%, 10% and 15% of purified water (by weight) were embedding

material for *B.burgdorferi* spirochetes. In this case Leica EM AFS2 programming with agitation device was done as:

Table 2.

Program view for Leica EM AFS2.

	T_{start} (°C)	T_{end} (°C)	Slope (°C/hour)	Time (hour)
1.	-82	-82	0	03:00
2.	-82	-28	5	10:48
3.	-28	-28	0	08:00
4.	-28	-20	8	01:00
5.	-20	-20	0	48:00

Dehydration with 90% acetone was in the step 1 and 2. After 2 series of 10 min wash with 90% ethanol, the acrylic resin with different water content was given in polypropylene flat bottom capsules sequentially with increasing concentration every 15 min. The step no.5 was provided for polymerization of acrylic resins with biological samples inside under the LED UV-lamp of Leica EM AFS2.

These two AFS devices were provided by the Laboratory of Electron Microscopy, Biology Centre of ASCR - Institute of Parasitology (Ceske Budejovice, Czech Republic). The main difference was in technical improvement of Leica EM AFS2 model that facilitate the work, as LED illumination in the chamber, user-friendly interface for programming and S6E stereomicroscope.

3.2.3 Sample sectioning

The polymerized blocks were freed from the form in which they were polymerized by a cut with a surgical scalpel in the case of polypropylene flat bottom capsules and immersion in a tub with warm water in the case of gelatin.

In present work for ultramicrotomy by Leica Ultracut UCT Ultramicrotome (Leica Microsystems, part of Danaher, Germany) were used self-prepared glass knifes. The glass knifes were made from the glass strips by LKB 7801 A Knife Maker (LKS Produkter KB, Sweden) with glass knife fork tool. The quality of the glass knife edge depends on the break speed, the slow speed normally provides the good edge of the one. It should be noted

that glass knife edge does not remain sharp for longer time, as diamond's one. Diamond knife could be used for calcified biological tissues and have good characteristics for cutting of thinner sections, as 10-20 nm thick.[57] The troughs were made by acrylate adhesive polyester film tape 850 Silver (3M, USA) and sealed by nail polish. The clearance angle was set as 6° for Leica Ultracut UCT Ultramicrotome knife holder.

To start with ultramicrotomy the block trimming was made by hand with double-edged razor blade at the angle about 60° to the vertical from all four sides forming a trapezoidal shape of the specimen block. It is necessary to monitor the trimming process, because deep riffles provoke the capillary process, when the liquid from the trough stretches after the block. The mechanical trimming of surface was done by Leica Ultracut UCT Ultramicrotome followed by sectioning on the trough with liquid (purified water or 10% actenone). Accompanied by interference phenomenon the floating sections help visually determine the thickness of the ones [Appx.4]. The movement directions during sectioning of mounted block is shown in Appx.5.

The motor cutting speed was 40-100 mm/s for surface mechanical trimming and 2 mm/s for the specimen thickness up to 90 nm as optimal one.

The specimen corrugation was partially reduced by chloroform wafting on a ear wand over the section.[48]

3.3 Study methods

Study methods in present work were aimed at suitability of derived embedding media for CLEM techniques. Micromechanical properties of epoxy, acrylic and aminoplastic resins were investigated by Micro Combi Tester (CSM Instrument, Switzerland) in the Laboratory of Morphology and Rheology of Polymer Materials, Otto Wichterle Centre of Polymer Materials and Technologies (Innovation center of the Institute of Macromolecular Chemistry, Academy of Sciences of the Czech Republic, Prague).

FLM examination was aimed at clarifying of incorporated fluorescent label availability in biological tissue in acrylic embedding media. The ultrastructure examination of the biological sample for ROI was done by TEM.

3.3.1 Measurement of micromechanical properties

The material hardness tests were done by Micro Combi Tester to determine the influence of crosslinking in the resin on the Leica Ultracut UCT Ultramicrotome sectioning process. The instrumented microhardness tests were done at RT by square base pyramid shaped indenter. The surface characterization was done by dint of LM NIKON/C73.

The study conditions for HPMA with 15% water content (polymerized by heat at 50°C), HPMA with 15% water content (polymerized by long-wave UV irradiation at -20°C during 48 hours in Leica EM AFS), Nanoplast Hard resin (stirred under 65°C and polymerized by heat at 60°C during 5 days) were the next: indenter depth 400 on the x axis and 0 on the y axis with standard load 490.5 mN for 6 s holding time. To determine the mean value 10 surface injections were done for each sample.

3.3.2 FLM

The biological sample, prepared for investigation (see 3.2.) was sectioned and 70-90 nm thick sections were given on the drop of 10% acetone on the microscope slides (Waldemar Knittel, Germany), some of them were investigated directly on the copper mesh grids for later research in TEM (to facilitate ROI finding). To stick these mesh grids to the microscope slide the drop of water was added on the glass surface. The microscope slide with sectioned biological sample was mounted to Olympus BX41 microscope (Olympus, Japan) for inspection. Excitations of UV (330-385 nm), blue (460-490 nm), green light (510-550 nm) and full spectrum light were used for detection and observation of GFP-expressing virulent derivative of *B.burgdorferi* Bb914 strain 297. The reflected light and sample fluorescence were viewed through the UMPlanFI objectives (Olympus, Japan) with followed magnifications: 5x/0.15 BD, 10x/0.30 BD, 20x/0.46 BD, 50x/0.80 BD, 100x/1.30 Oil. Immersion oil drop was given on the second cover microscope slide during observation under UMPlanFI 100x/1.30 Oil objective.

3.3.3 TEM

The *B.burgdorferi* 30-100 nm thick sections were studied by TEM for ROI ultrastructure examination. The water-miscible embedding media were also studied for their stability under self-biasing tungsten filament in JEOL JEM-1010. For one of the experiments,

100 nm thick section of HPMA (Fluka, BioChemika, Sigma-Aldrich Chemie GmbH, Switzerland) contained 10% water and polymerized by long-wave UV irradiation at -20°C, 30 nm thick sections of HPMA (Electron Microscopy Sciences, USA) contained 15% water and polymerized by long-wave UV irradiation at -20°C and 30 nm HPMA (Electron Microscopy Sciences, USA) contained 15% water and polymerized by 50°C heat were carbon coated by JEOL JEE 4C vacuum evaporator to provide resin stability under the electron beam.

CHAPTER 4. RESULTS

In the course of the experiments I carried out the following tasks:

1. Subjectively evaluate the ability of water-miscible embedding media to be cut by Leica Ultracut UCT Ultramicrotome.
2. Estimate the micromechanical properties of epoxy, acrylic and aminoplastic embedding media and determine the presence of changes over time in micromechanical properties of water-miscible embedding medium by Micro Combi Tester.
3. Check the stability of water-miscible embedding media under tungsten filament in JEOL JEM-1010 TEM.
4. Detect GFP-expressing virulent derivative of *B.burgdorferi* Bb914 strain 297 and register its location (ROI) by Olympus BX41 microscope.
5. Detect ROI and examine its ultrastructure by JEOL JEM-1010 TEM, compare with results obtained by Olympus BX41 microscope.

4.1 The composition of the FS solution

Minimal extraction of cell components followed by good preservation of fine structure attributed to acetone, while methanol could substitute even with small presence of water and do it faster than acetone.[59]

That is why the FS program with shorter time was set up for agitation device with methanol reagent (see 3.2.2).

4.2 Polymerization results and sample sectioning

In present work I polymerized epoxy, acrylic and amino resins under different conditions of heat and UV, as temperature and time of curing, to determine the suitable polymerization mode for its application in CLEM.

The bacterial culture was embedded in the hard resins to obtain the uniform thin section layer for EM observation. To facilitate the task for ROI identification I used one section for sequential observation in FLM and TEM.

It should be noted that patience during sample sectioning and careful attitude to the obtained sections process increase the success result.

4.2.1 Water-miscible embedding media

In the Ref. 60 these media are indicated as possessing good cutting properties for all kinds of tissues and one of the main tasks of present work was to test their cutting properties experimentally.

4.2.1.1 Hydroxypropyl Methacrylate

During my study I used two different hydroxypropyl methacrylate kits, the one was produced by Sigma-Aldrich Chemie GmbH, Switzerland and another one by EMS, USA. The polymerization results, which I obtained during the study are based on my subjective assessment and presented in the Table 3 and Table 4.

Table 3

Polymerization results according to percentage of imparted water for HPMA (Fluka, BioChemika, Sigma-Aldrich Chemie GmbH, Switzerland)

% of imparted water	Presence of a biological sample	Polymerization mode	Result
1	*2*	*3*	*4*
5	none	55°C heat for 48 hours	The resin block had low hardness with air bubbles in thickness.
5	*B.burgdorferi* with QDs	long wave UV irradiation at -20°C for 60 hours	I got with effort only 200 nm thick sections.
5	*B.burgdorferi*	long wave UV irradiation at -20°C for 60 hours	I got with effort the ribbon of 200 nm thick sections.

1	*2*	*3*	*4*
			The brittle 80 nm thick sections I got at 3 mm/s cutting speed.
10	none	55°C heat for 48 hours	The resin block had low hardness.
10	none	long wave UV irradiation at -20°C for 48 hours	The resin block was flexible as a rubber.
10	*B.burgdorferi*	long wave UV irradiation at -20°C for 48 hours (with methanol freeze-substitution medium; agitation device in AFS protocol)	After resin polymerization in the lower part of polypropylene flat bottom capsules was detected the presence of air.
10	none	long wave UV irradiation at -20°C for 60 hours	The resin block had sensitive surface to mechanical action (squeezing with mounting clamps), but the resin sliced gently.
15	none	50°C heat for 48 hours	The resin was not polymerized (liquid state).
15	none	55°C heat for 48 hours	The resin block was not polymerized completely and was sticky to the touch.
15	none	long wave UV irradiation at -20°C for 48 hours	The resin block had milky color and was flexible as a rubber.
15	none	long wave UV irradiation at -20°C for 60 hours	The resin block had white color precipitate in the bottom.

Table 4

Polymerization results according to percentage of imparted water for HPMA (EMS, USA)

% of imparted water	Presence of a biological sample	Polymerization mode	Result
1	*2*	*3*	*4*
5	*B.burgdorferi*	long wave UV irradiation at -20°C for 48 hours (with methanol freeze-substitution medium; agitation device in AFS protocol)	The resin block had air bubbles at the bottom.
10	none	50°C heat for 48 hours	The resin was not polymerized (liquid state).
10	none	long wave UV irradiation at -20°C for 48 hours	The resin was not polymerized (liquid state).
10	*B.burgdorferi*	long wave UV irradiation at -20°C for 48 hours (with acetone to ethanol freeze-substitution medium; agitation device in AFS protocol)	I got fragile 200 nm thick sections, while 80 nm thick sections I got at 10 mm/s cutting speed.
10	*B.burgdorferi*	long wave UV irradiation at -20°C for 48 hours (methanol freeze-substitution medium)	I got 90 nm thick sections at 2 mm/s cutting speed, these sections were clung to the edge of the glass knife. The 80 nm thick sections I got at 10 mm/s cutting speed. To prevent chatter appearance I reduced the cutting speed to 2 mm/s and got 70 nm sections,

1	*2*	*3*	*4*
			which were stretched from the edge of the glass knife with simultaneous adhesive phenomenon.
15	none	55°C heat for 48 hours	The resin block had low hardness, I easily formed the block face. The resin block had a lot of small bubbles inside, I detected it visually during block trimming. The sections 400 nm thick I got at 50 mm/s cutting speed. During the block trimming the resin created fibers on the edge of the glass knife.
15	none	long wave UV irradiation at -20°C for 48 hours	The resin block was milky color, was flexible as a rubber and contained air bubbles in thickness.
15	none	long wave UV irradiation at -20°C for 60 hours	The resin block trimming was difficult due to cleavages. The sections adhered to the glass knife edge. During sectioning resin block cracked and deep holes in resin thickness indicated presence of air during the polymerization process.

4.2.1.2 Glycol Methacrylate

The glycol methacrylate polymerization results are presented in the Table 5.

Table 5

Polymerization results according to percentage of imparted water for GMA (low acid) (EMS, USA)

% of imparted water	Presence of a biological sample	Polymerization mode	Result
1	*2*	*3*	*4*
3	none	55°C heat for 48 hours	The resin block was polymerized.
3	none	long wave UV irradiation at -20°C for 48 hours	The resin block was polymerized.
6	none	55°C heat for 48 hours	The resin block was polymerized.
6	none	long wave UV irradiation at for 48 hours	The resin block was polymerized.
9	none	55°C heat for 48 hours	The resin had matt surface.
9	none	long wave UV irradiation at -20°C for 48 hours	The resin was not transparent in thickness.
9	*B.burgdorferi*	long wave UV irradiation at -20°C for 48 hours (methanol freeze-substitution medium, last infiltration step in AFS protocol had 5% of water in methanol)	During the section ribbon formation the resin did not float out on the water in trough and clung to the edge of the glass knife. Under these conditions I got 80 nm sections at 10 mm/s cutting speed. The resin sections were wavy with uneven thickness.
9	none	long wave UV irradiation at -20°C for 60 hours	The resin block trimming was difficult due to cleavages. The resin block had sensitive surface

1	*2*	*3*	*4*
			(squeezed in mounting clamps). The sections was cut gently, during the block trimming I got 20 nm thick sections, but they were uneven and irregular in thickness.

4.2.1.3 Polyethylene Glycol – Glycol Methacrylate mix

Table 6

Polymerization results according to percentage of imparted water for GMA/PEG (1% v/v) (EMS, USA)

% of imparted water	**Presence of a biological sample**	**Polymerization mode**	**Result**
1	*2*	*3*	*4*
3	none	50°C heat for 48 hours	The resin block was polymerized.
3	none	long wave UV irradiation at -20°C for 48 hours	The resin block was polymerized.
6	none	50°C heat for 48 hours	The resin block was polymerized.
6	none	long wave UV irradiation at -20°C for 48 hours	The resin block was polymerized.
9	none	50°C heat for 48 hours	The resin block was hard to trim due to its solid consistency, cleavages appeared. Simultaneously the resin block had sensitive surface (squeezed in mounting clamps). The resin sections in the trough with 10% acetone were sticky, had small tension and were easily cut by fine hair.

1	*2*	*3*	*4*
9	none	long wave UV irradiation at -20°C for 60 hours	I got 50 nm, 100 nm thick sections.

4.2.1.4 Nanoplast

Nanoplast resin samples after 60°C heat polymerization during 72 hours with silica gel as dessicant in the oven had slightly wet surface and air bubbles at the bottom of the resin blocks.

4.2.2 Lowicryl K4M

One of three Lowicryl K4M resin samples was polymerized by long wave length UV for 24 hours at -35°C followed by 6 days of natural UV polymerization at -6°C to 2°C at open space, the resin block had matt pinkish color.

4.2.3 LR White

LR White is an aromatic acrylic resin mixture with $8 \cdot 10^{-3}$ Pa viscosity rate, low toxicity and stability under the electron beam.[61] To confirm the last statement this resin was prepared for microindentation hardness test investigation.

This resin is universal for wide scale of polymerization types: heat, UV irradiation, chemical and microwave one. In present study I used heat and long wave UV irradiation at -20°C for polymerization.

Table 7

Polymerization results according to polymerization mode for LR White (EMS, USA)

Presence of a biological sample	**Polymerization mode**	**Result**
1	*2*	*3*
None	51°C heat for 48 hours	The resin block was slightly damp and sticky-apparently it was insufficiently polymerized.
None	60°C heat for 48 hours	During the resin block trimming I got relatively easy 500 nm thick sections at 40 mm/s cutting speed.

1	*2*	*3*
none	long wave UV irradiation at -20°C for 24 hours	The resin block had matt surface.
none	long wave UV irradiation at -20°C for 48 hours	The resin block had matt surface.

4.2.4 EMbed 812

EMS (USA) have replaced EPON 812 by Embed 812 in 1978. The resin block was fully polymerized at 60°C heat during 24 hours. This resin was prepared for microindentation hardness test investigation to verify the manufacturer's declaration of cutting qualities and stability under the electron beam. [56]

4.3 Measurement of micromechanical properties

The hardness number was calculated using test load, impression length and Vickers indenter shape factor.[56]

EMbed 812 and LR White were polymerized by heat at 60°C for 24 hours and 48 hours respectively and the tested surface was sufficiently smooth (obtained by block trimming in Leica Ultracut UCT Ultramicrotome) and reflective to prevent artefacts during microindentation hardness testing. The changes in indentation hardness and indentation modulus over time were investigated.

To achieve required smoothness of tested surface the down stroke speed of specimen arm was manually configured as 100-50-20-5-2 mm/s for 500 nm sections of Embed 812, during the block trimming. Surface touching was avoided. Block trimming of LR White was done by 100-40 mm/s specimen arm down stroke speed for 500 nm sections.

The surface finish had influence on the measurement, small chips created air pits where indenter lied by value, H_{IT} was more than 400 MPa.

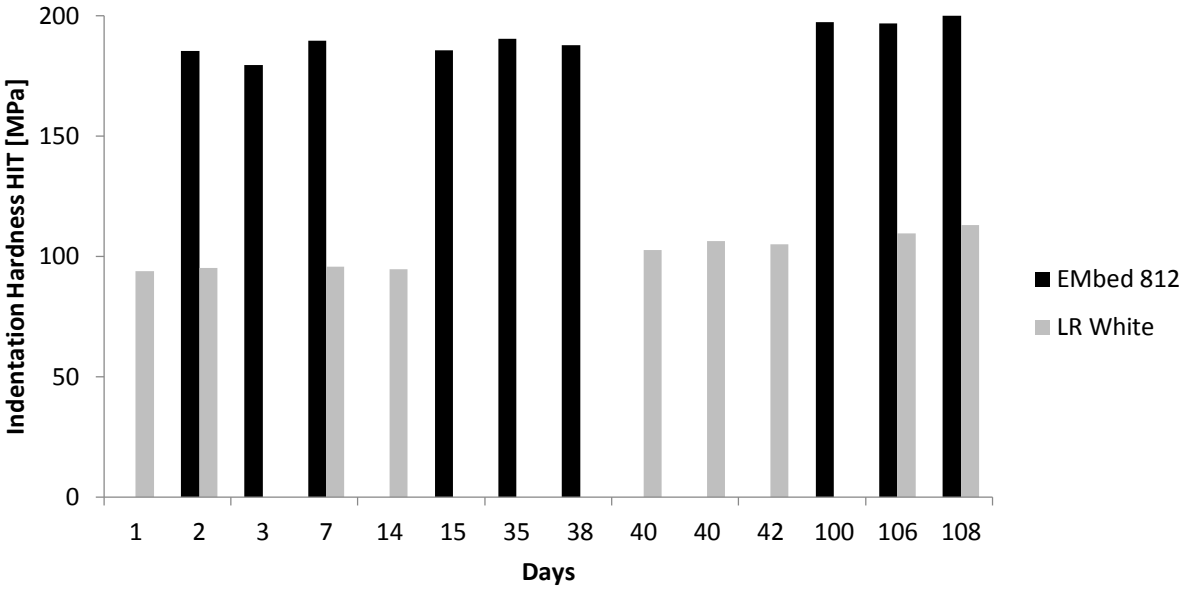

Figure 13. Indentation hardness H_{IT} changes over time. [based on Ref. 62]

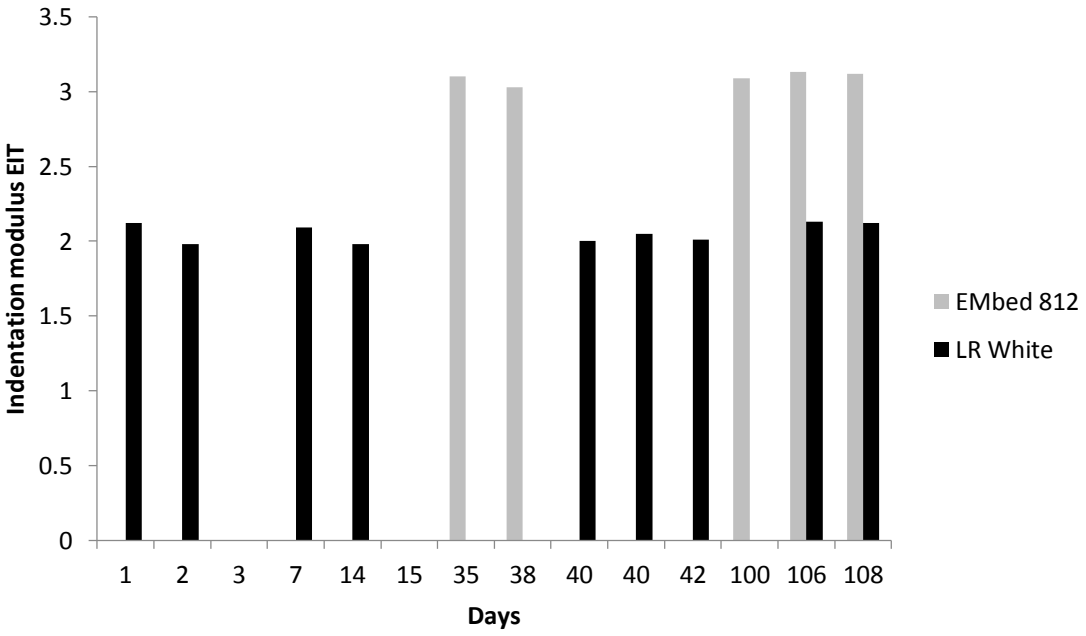

Figure 14. Indentation modulus E_{IT} changes over time. [based on Ref. 62]

From Fig.13 and Fig.14 Embed 812 is harder and inflexible than LR White, in process of time this phenomenon becomes more characteristic.

For measurement of micromechanical properties by Micro Combi Tester it was necessary to prepare the 2×2 mm block of HPMA (EMS, USA) with 15% water content, polymerized during 48 hours by 55°C heat. To avoid measurement error I decided to get the smooth surface of the block by trimming in Leica Ultracut UCT Ultramicrotome. But required size of the block was impossible to infix in the specimen holder; if I used a foil for its reinforcement inside, the wavy surface with compressed areas was caused by block vibrations. In this case I decided to use the standard size of resin block (polished surface diameter was 7.92 mm). The indentation hardness H_{IT} of this resin by Micro Combi Tester was 100 MPa at 25000 mN/min indenter speed and after 6 month 198 MPa at 2500 mN/min indenter speed, which proves the solidification over time.

The same resin, polymerized in Leica EM AFS by long wave UV irradiation at -20°C for 48 hours had indentation hardness H_{IT} by Micro Combi Tester 196.3 MPa at 25000 mN/min indenter speed and after 6 month 215.6 MPa at 2500 mN/min indenter speed, which proves the solidification over time.

Nanoplast Hard had indentation hardness H_{IT} by Micro Combi Tester 334,5 MPa at 2500 mN/min indenter speed after 6 month of storage.

4.4 FLM examination

All obtained resin blocks were stored in aluminum foil in light-proof boxes at the refrigerator (4°C) to protect the GFP from UV light, to postpone the inevitable changes in their properties.

Table 8

Results of GFP detection in *B.burgdorferi* by Olympus BX41 microscope

Embedding resin	% of imparted water	Polymerization mode	Section thickness (nm)	GFP visibleness
HPMA (Fluka, BioChemika, Sigma-Aldrich Chemie GmbH, Switzerland)	5	Long wave UV irradiation at -20°C for 48 hours	200	The fluorescence signal was not detected.
HPMA (EMS, USA)	5	Long wave UV irradiation at -20°C for 48 hours (methanol freeze-substitution medium)	80 (10 mm/s specimen arm down stroke speed)	The fluorescence signal was not detected.
HPMA (EMS, USA)	5	Long wave UV irradiation at -20°C for 48 hours (acetone to ethanol freeze-substitution medium)	80	The fluorescence signal was not detected. I was not able to focus the image by 50x/0.80 BD UMPlanFI objective.
HPMA (EMS, USA)	10	Long wave UV irradiation at -20°C for 48 hours	80	The fluorescence signal was not detected.

4.5 TEM examination

It should be noted that to reduce chatter I tried to change cutting down stroke speed in Leica Ultracut UCT Ultramicrotome, but this does not overcome it completely. It was not possible to change the sectioning angle due to capillary process, which greatly complicates the sectioning by Leica Ultracut UCT Ultramicrotome.

Table 9

Observation results of *B.burgdorferi* by JEOL JEM-1010 microscope

Embedding resin	**% of imparted water**	**Presence of a biological sample**	**Polymerization mode**	**Section thickness (nm)**	**Accelerating voltage (kV)**	**Observation results**
1	*2*	*3*	*4*	*5*	*6*	*7*
HPMA (Fluka, BioChemika, Sigma-Aldrich Chemie GmbH, Switzerland)	5	*B.burgdorferi*	long wave UV irradiation at -20°C for 48 hours (acetone to ethanol freeze-substitution medium)	80, 90	80	The resin sections had chatter. During the observation with simultaneous presence of stable regions the sections had been exploded.

1	*2*	*3*	*4*	*5*	*6*	*7*
HPMA (Fluka, BioChemika, Sigma-Aldrich Chemie GmbH, Switzerland)	10	none	long wave UV irradiation at -20°C for 48 hours	100 (with thin carbon layer)	80	The resin sections were stable under electron beam without any tears.
HPMA (EMS, USA)	5	*B.burgdorferi*	long wave UV irradiation at -20°C for 48 hours (methanol freeze-substitution medium)	60, 80 (10 mm/s specimen arm down stroke speed)	80	The resin sections were relatively stable under the electron beam. I was not able to get not blurred image of spirochetes, so its morphological structure was not possible to get in this type of embedding media. The resin sections had chatter on a whole observed sample except the area with spirochetes group.

1	*2*	*3*	*4*	*5*	*6*	*7*
HPMA (EMS, USA)	5	*B.burgdorferi*	long wave UV irradiation at -20°C for 48 hours (methanol freeze-substitution medium)	70 (2 mm/s specimen arm down stroke speed)	80	I was not able to get not blurred image of spirochetes, so its morphological structure was not possible to get in this type of embedding media. The resin sections had chatter on a whole observed sample including the area with spirochetes group (Fig. 7). The resin sections were partially torn.
HPMA (EMS, USA)	10	*B.burgdorferi*	long wave UV irradiation at -20°C for 48 hours (methanol freeze-substitution medium)	90	60	I was not able to focus the image, The resin section ruptured under the electron beam.
HPMA (EMS, USA)	10	*B.burgdorferi*	long wave UV irradiation at -20°C for 48 hours (methanol freeze-substitution medium)	80, 90 (10 mm/s specimen arm down stroke speed)	80	The resin sections were stable under the electron beam, only appeared the breaks at the specimen grid edges (Fig. 8, 9). At low magnifications the

1	*2*	*3*	*4*	*5*	*6*	*7*
						spirochetes had sufficiently clear contours (Fig. 10).
HPMA (EMS, USA)	15	none	50°C heat for 48 hours	80	80	The resin sections had chatter (Fig. 11), the focused electron beam provoked rupture of the resin section and its corrugation.
HPMA (EMS, USA)	15	none	55°C heat for 48 hours	30	80	The resin section ruptured and folded under the electron beam.
HPMA (EMS, USA)	15	none	55°C heat for 48 hours	30 (with thin carbon layer)	80	The resin sections were stable under the electron beam.
HPMA (EMS, USA)	15	none	long wave UV irradiation at -20°C for 60 hours	30	80	The resin sections had chatter which indicated variation in section thickness (Fig. 12). The resin section ruptured and folded under the electron beam.
HPMA (EMS, USA)	15	none	long wave UV irradiation at -20°C for 60 hours	30 (with thin carbon layer)	80	The resin sections were stable under the electron beam.

1	*2*	*3*	*4*	*5*	*6*	*7*
HPMA (EMS, USA)	15	none	long wave UV irradiation at -20°C for 60 hours	80	80	The resin sections had chatter which indicated variation in section thickness.

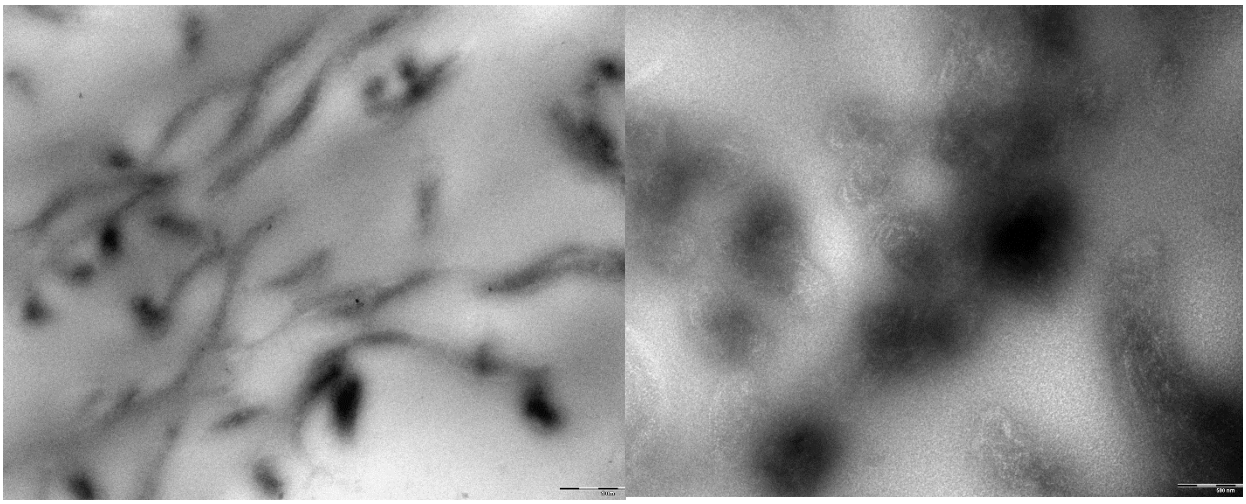

a) b)

Figure 7. 70 nm thick section with *B.burgdorferi* polymerized in HPMA (EMS, USA) with 5% of imparted water under long wave UV irradiation at -20°C for 48 hours (methanol freeze-substitution medium) in JEOL JEM-1010 microscope under accelerating voltage 80 kV. Scale bar: a) 1 µm, b) 500 nm.

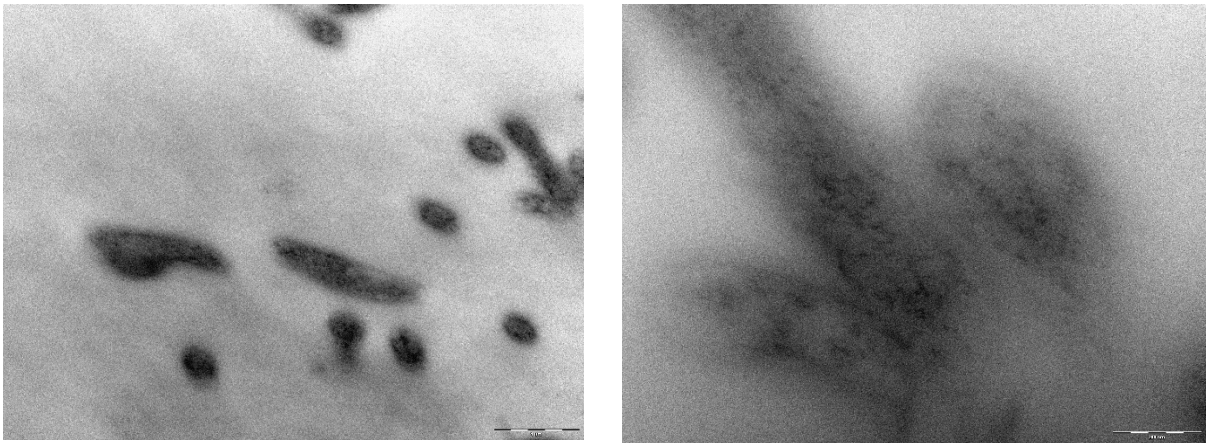

a) b)

Figure 8. 80 nm thick section with *B.burgdorferi* polymerized in HPMA (EMS, USA) with 10% of imparted water under long wave UV irradiation at -20°C for 48 hours (methanol freeze-substitution medium) in JEOL JEM-1010 microscope under accelerating voltage 80 kV. Scale bar: a) 1 µm, b) 200 nm.

a) b)

Figure 9. 90 nm thick section with *B.burgdorferi* polymerized in HPMA (EMS, USA) with 10% of imparted water under long wave UV irradiation at -20°C for 48 hours (methanol freeze-substitution medium) in JEOL JEM-1010 microscope under accelerating voltage 80 kV. Scale bar: a) 20 µm, b) 500 nm.

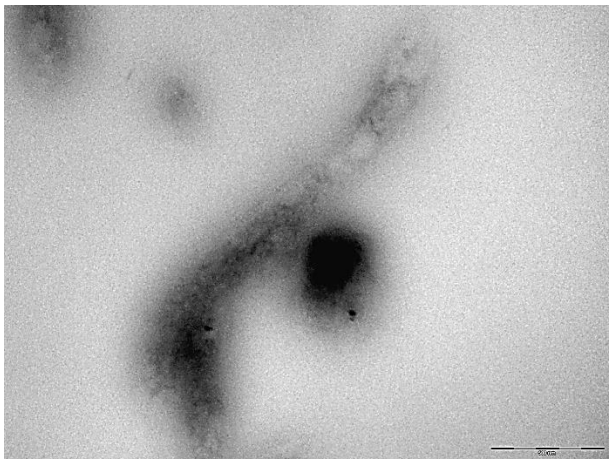

Figure 10. 80 nm thick section with *B.burgdorferi* polymerized in HPMA (EMS, USA) with 10% of imparted water under long wave UV irradiation at -20°C for 48 hours (methanol freeze-substitution medium) in JEOL JEM-1010 microscope under accelerating voltage 80 kV. Scale bar: 500 nm.

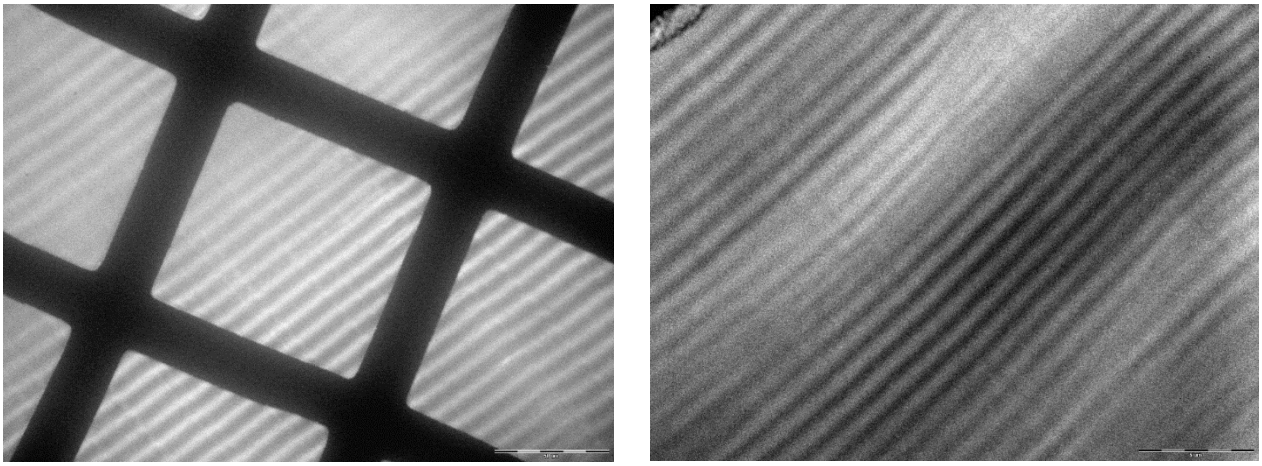

a) b)

Figure 11. 80 nm thick HPMA (EMS, USA) section with 15% of imparted water under 50°C heat polymerization for 48 hours in JEOL JEM-1010 microscope under accelerating voltage 80 kV. Scale bar: a) 50 µm, b) 5 µm.

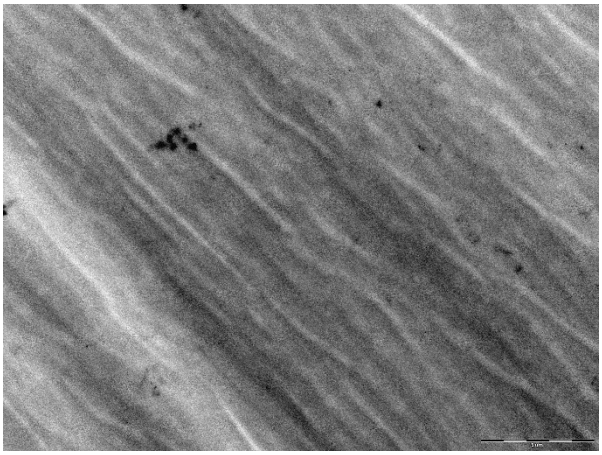

Figure 12. 30 nm thick HPMA (EMS, USA) section with 5% of imparted water under long wave UV irradiation at -20°C for 60 hours in JEOL JEM-1010 microscope under accelerating voltage 80 kV. Scale bar: 5 µm.

CHAPTER 5. DISCUSSION

The one of the most perspective methods to study biological objects at the cellular level is the CLEM technique.

Fluorescent markers are able to image the live cells, while ultrastructure morphology of a biological object in EM usually obtains in high vacuum conditions. The differences in sample preparation protocols for LM and EM create certain difficulties for precise correlation in LM and EM imaging. In this case for relocation of ROI the TEM finder grids are used or cell position in the section is taking into account.[63] The biological sample must be fixed, dehydrated and embedded into resin with the possibility that GFP will reduce the fluorescence due to protonation of GFP chromophore during embedding process.[64] Because imaging is very important research tool in natural sciences, the preparation methods for post-embedding CLEM technique, which are not contradicting each other, are still the trial area.

To keep the fluorescence intensity during resin embedding I used the buffer solution with pH=7,2 as reported in the Ref. 50, because chromophore "protonation state […] is responsible for GFP pH sensitivity"[35].

To study possibility of water-miscible embedding media utilization for accurate correlation in FLM and TEM I used hydroxypropyl methacrylate with 5 and 10 percent of imparted water, with different condition of long wave UV polymerization for embedded *B.burgdorferi*, where composition of FS solution was changed to ethanol[5] as the second fixative or have been replaced by methanol. According to Johnson E. et al. ethanol did not affect in-resin fluorescence and resin sections have less tears then.[65]

HPMA resin is hydrophilic one and this characteristic may preserve the fluorescence in the embedded biological material[66] because fluorescent proteins "maintain their conformation in hydrated states"[67], in addition Yang Zh. et al. represents HPMA as an ideal media for fluorescence preservation.[67]

I was not successful in the fluorescent signal observation during my experiments. I atribute it to the way of manipulating with *B.burgdorferi* that it was not kept in the dark and during sectioning by Leica Ultracut UCT Ultramicrotome the sections with embedded *B.burgdorferi* were illuminated by internal bulb of the device (it is not possible to make this procedure in the

dark, because the quality of the resin section and its thickness is controlled visually and by light reflection from the resin section).

My experiment with GFP detection in Olympus BX41 microscope probably led to "bleaching" of the fluorescence, because I used full spectrum light (to find the section on the grid) and sequential switching of UV (330-385 nm), blue (460-490 nm), green light (510-550 nm) to be sure that I detected specifically GFP signal

I used the resin embedding protocol where heavy metals were absent to prevent fluorescence quenching but simultaneously led to low contrast.[68]

In freeze substitution protocol I added 2% GA in the substitution media, that purposed by Bell K. et al. as excellent ultrastructural preservation without GFP fluorescence elimination, but with simultaneous increasing of autofluorescence of plant cell components.[69] I took this statement into account, since endogenous expression is the same for live plant or animal cell.[51]

Because preliminary identification of *B.burgdorferi* through Olympus BX41 microscope was unsuccessful, I had huge amount of spirochetes in the square meshes of TEM standard grid without marks to study its ultrastructure by JEOL JEM-1010 TEM and I was not able to find the corresponding cells. I was not able to focus the image and blurred silhouettes of *B.burgdorferi* did not allow me to get ultrastructure information. Despite I used the protocol, based on manufacturer's recommendations[51, 60] for preserving a recordable GFP signal and get good image resolution in EM, I was not able to make the correlation at all.

The blurred image of spirochetes during observation under the electron beam in JEOL JEM-1010 TEM probably points on atomic structure scattering potential,[70] because the embedding material was hydrophilic.

80 nm thick section with *B.burgdorferi* polymerized in HPMA (EMS, USA) with 10% of imparted water under long wave UV irradiation at -20°C for 48 hours (methanol freeze-substitution medium) under accelerating voltage 80 kV revealed the presence of sufficiently clear spirochete contours, but to get the ultrastructure image still was not possible.

At the same time JEOL JEM-1010 TEM gave me the opportunity to check the stability of water-miscible embedding media with different percentage of imparted water, different polymerization modes and different thickness under tungsten filament at 60 kV, 80 kV accelerating voltage. I noted that the biological material embedded in hydroxypropyl methacrylate

sections with thickness ≤90 nm tends to tear under the electron beam, most often in the center of the TEM grid mesh, that complicated my study. Especially, if the ROIs were directly in the in the field of discontinuity.

To find a possible cause of ruptures in the embedding medium itself, I have coated few hydroxypropyl methacrylate sections (with different thickness (30 nm, 100 nm) and different water percentage (15 and 10% resp.)) with carbon film by JEOL JEE 4C vacuum evaporator. TEM imaging showed that the resin surface was not contaminated with coarse carbon particles, due the fact that I conducted the carbon atomization by indirect method, when the deposition surface was hidden from direct hit of carbon atoms including accidental cleavage of large particles from the carbon spike. As the result, I got stable resin sections, without any tears. These sections did not contained any biological material, but resin blocks were polymerized by long wave UV irradiation at -20°C for 60 hours and 48 hours resp., which makes it possible to use this protocol for biological sample embedding.

Rupture of hydroxypropyl methacrylate sections with embedded *B.burgdorferi* inside was not prolonged process, after abrupt tearing - it stopped, and partially spatially undistorted material was at mesh edges and it does not changed upon further study, even after prolonged storage in the refrigerator at 4°C.

It should be noted that the common problem of observed sections was chatter, that makes it possible to misinterpret the information about the ultrastructure of the biological object. I attribute this to the difficulties during sample sectioning with Leica Ultracut UCT Ultramicrotome, created by the structure of embedding media and the capability of the equipment, when the block face on my opinion slightly warms up during mechanical shearing. Polymerization mode did not affect the occurrence of chatter, I watched it both: in samples polymerized by heat conditions and samples, polymerized by UV irradiation.

To secure the resin block in the socket of specimen arm I tried to lay a piece of aluminum film wrapped around the base of the resin block, despite the manufacturer has provided a toothed mounting surface. This improvement did not lead to the desired result, in some cases there was an imbalance of clamping, the resin block could suddenly deviate upwards at the junction with the edge of the glass knife, that threatened to break the resin block and violate the whole process of sectioning.

In order to obtain sections with uniform thickness I had changed the motor cutting speed to the lowest possible value, but I spent a lot of time to get each section. Since my experience has shown that very low motor speed complicated the work at all – hydrophilic attitude of acrylic resins attracted the water from the trough.

The section corrugation was not effectively relieved by chloroform wafting on a cotton swab over the section. I attribute this to the internal structure of the resin block, modified by water content in it and respectively by the type of polymerization.

B.burgdorferi immunolabeled with QDs was kindly provided by Jana Kopecká (Laboratory of Electron Microscopy, Biology Centre ASCR - Institute of Parasitology, 2015) I embedded this sample in HPMA (Sigma-Aldrich Chemie GmbH, Switzerland) with 5 % of imparted water, and I used for the polymerization long wave UV irradiation at -20°C for 60 hours. This sample was hard to cut less than 200 nm thick sections, than the sample without QDs, despite the fact that QDs are good as optical contrast agents.[71]

The HPMA of this manufacturer had the tendency to stay liquid after 50°C heat polymerization during 2 days, when I added 15% of water to hydroxypropyl methacrylate, probably due to limits of HPMA to be mixed with water[51]. The same problem appeared in HPMA embedding kit from EMS, USA, but with 10% of imparted water, it was not polymerized.

GMA (low acid) (EMS, USA) had been polymerized at the 55°C heat and long wave UV at -20°C during 2 days, with presence of 3 % -9 % of imparted water. But it was hard to get uniform section surface during resin block trimming. The same behavior I detected from GMA/PEG (1% v/v) (EMS, USA). According to the obtained results the higher percentage of imparted water in GMA/PEG (1% v/v) (EMS, USA) under long wave UV irradiation at -20°C for 60 hours results in ability to get the section even 50 nm thick.

It should be noted that for the purpose of experiment, I added 5% of water in methanol in the last infiltration step in AFS protocol for GMA (low acid) (EMS, USA) with 9% of imparted water and presence of *B.burgdorferi*, then I polymerize it with long wave UV irradiation at -20°C for 48 hours. The presence of water in the last infiltration step does not affected the polymerization success but complicated the sectioning by Leica Ultracut UCT Ultramicrotome.

The resin block of HPMA (EMS, USA) with 10% of imparted water and embedded *B.burgdorferi* before polymerization under long wave UV irradiation have passed the stage of fast

FS in Leica EM AFS2 that was done by agitation device. As the result I got the fragile sections, that may be the result of vertical position of polypropylene capsules inside the Leica EM AFS2 chamber, while McDonald K.L. et al. insists that polypropylene capsules should be located close to horizontal position for good mixing of the FS solution.[72]

Taking into account all the experimental data obtained, I can confirm, that adding water into the polymer gives success in polymerization in 75,8% of cases for acrylic resins.

CHAPTER 6. CONCLUSIONS

- Adding water to the polymer during hydrophilic resin preparation eventually led to deterioration of resin cutting abilities with Leica Ultracut UCT Ultramicrotome.
- The sections of acrylic resins with percentage of imparted water had chatter, which was not able to get rid of.
- The embedding protocols for HPMA with 5-15% of imparted water, which are presented in this study, do not led to preserve a recordable GFP signal in *B.burgdorferi.*
- The sections of water-miscible resins with 5 % - 15% of imparted water were unstable under the electron beam in JEOL JEM-1010 TEM and did not allow to focus the blurred image of *B.burgdorferi.*
- Use of agitation device during FS protocol accelerates the infiltration process, the resin blocks were succesfully polymerized.

REFERENCES

1. ROBINSON, J.M.; VANDRÉ D.D. (1997) Efficient immunocytochemical labeling of leukocyte microtubules with fluoronanogold: an important tool for correlative microscopy. Journal of Histochemistry & Cytochemistry 45 (5): 631-642. DOI: https://doi.org/10.1177/002215549704500501.
2. ROBINSON, J. M.; TAKIZAWA T.; VANDRÉ D.D. (2000) Applications of gold cluster compounds in immunocytochemistry and correlative microscopy: comparison with colloidal gold. Journal of Microscopy, 199(3): 163-179. Review. PubMed PMID: 10971797.
3. NOGALES E.; SCHERES S.H.W. (2015) Cryo-EM: A unique tool for the visualization of macromolecular complexity. Molecular cell. 58(4): 677-689. DOI:10.1016/j.molcel.2015.02.019.
4. delmic [online]. SECOM. Ultrastructure in the Spotlight [cit. 11.12.2017]. Available on WWW: <http://www.delmic.com/secom>.
5. delmic [online]. DELPHI. Insight simplified [cit. 11.12.2017]. Available on WWW: <http://www.delmic.com/delphi>.
6. FEI [online]. MAPS & CorrSight : Non-integrated correlative workflow [cit. 11.12.2017]. Available on WWW: <https://www.fei.com/life-sciences/cellular-biology/correlative-microscopy/>.
7. Hitachi High-Technologies GLOBAL [online]. Launch of the MirrorCLEM system for correlative light and electron microscopy [cit. 11.12.2017]. Available on WWW: <http://www.hitachi-hightech.com/global/about/news/2016/nr20160721.html>.
8. Nanounity [online]. Correlative Microscopy. The SECOM platform integrates fluorescence microscopy and SEM [cit. 11.12.2017]. Available on WWW: <http://www.nanounity.com/correlative-microscopy.php>.
9. SPRING, K.R.; DAVIDSON M.W. Introduction to Fluorescence Microscopy [online]. Nikon MICROSCOPYU [cit. 11.12.2017]. Available on WWW: < https://www.microscopyu.com/techniques/fluorescence/introduction-to-fluorescence-microscopy>.

10. ELLINGER, P. (1940) Fluorescence microscopy in biology. Biological Reviews, 15(3): 323-347.
11. BOGDANOV, A.M.; BOGDANOVA, E.A.; CHUDAKOV, D.M.; GORODNICHEVA, T.V.; LUKYANOV, S.; LUKYANOV, K.A. (2009) Cell culture medium affects GFP photostability: a solution. Nat. Methods, 6: 859–860. DOI: 10.1038/nmeth1209-859.
12. PAWLIZAK, S. Fluorescence Microscopy [online]. University of Leipzig. Soft matter physics division [cit. 11.12.2017]. Available on WWW: < http://home.uni-leipzig.de/pwm/web/?section=introduction&page=fluorescence>.
13. СТОЙКОВА, Е.Е.; ПОРФИРЬЕВА, А.В.; ЕВТЮГИН, Г.А. Анализ следовых количеств веществ. Казань: Казанский (Приволжский) федеральный университет, 2010. pp. 72.
14. WOLNIAK, S.M. Principles of microscopy [online]. University of Maryland. Department of cell biology & molecular genetics [cit. 11.12.2017]. Available on WWW: < http://www.life.umd.edu/cbmg/faculty/wolniak/wolniakmicro.html>.
15. JEOL [online]. Transmission Electron Microscope (TEM). The difference between Electron Beam and Light [cit. 11.12.2017]. Available on WWW: < http://www.jeol.co.jp/en/science/em.html#Page1>.
16. Laboratory of Electron Microscopy [online]. Equipment [cit. 11.12.2017]. Available on WWW: < http://triton.paru.cas.cz/old-lem/equipment.php>.
17. CORTESE, K.; DIASPRO, A.; TACCHETTI, C. (2009) Advanced correlative light/electron microscopy: current methods and new developments using Tokuyasu cryosections. J. Histochem. Cytochem. 57: 1103–1112. DOI: 10.1369/jhc.2009.954214.
18. MIELAŃCZYK, L.; MATYSIAK, N.; KLYMENKO, O.; WOJNICZ, R. (2015) Transmission Electron Microscopy of Biological Samples. The Transmission Electron Microscope - Theory and Applications. InTech, chapter 9. pp.193-239. DOI: 10.5772/59457.
19. CORTADELLAS, N.; GARCIA, A.; FERNÁNDEZ, E. (2012) Transmission electron microscopy in cell biology: sample preparation techniques and image information. The handbook of instrumental techniques of the scientific and technological centers of the University of Barcelona (CCiTUB), BT.2. pp. 1-11.

20. LIDKE, D.S.; LIDKE, K.A. (2012) Advances in high-resolution imaging – techniques for three-dimensional imaging of cellular structures. J. Cell Sci. 125: 2571–2580. DOI:10.1242/jcs.090027.

21. van DRIEL, L.F.; KNOOPS, K.; KOSTER, A.J.; VALENTIJN, J.A. (2008) Fluorescent labeling of resin-embedded sections for correlative electron microscopy using tomography-based contrast enhancement. J. Struct. Biol. 161(3): 372-383. DOI: 10.1016/j.jsb.2007.09.021.

22. van BELLEGHEM., F.; CUYPERS, A.; SEMANE, B.; SMEETS, K.; VANGRONSVELD, J.; D'HAEN, J.; VALCKE R.. (2007) Subcellular localization of cadmium in roots and leaves of Arabidopsis thaliana. New Phytol. 173: 495–508. DOI: 10.1111/j.1469-8137.2006.01940.x.

23. PARK, J.; PARK, H.; ERCIUS, P.; PEGORARO, A.F.; XU, C.; KIM, J.W.; HAN, S.H.; WEITZ, D.A. (2015) Direct Observation of Wet Biological Samples by Graphene Liquid Cell Transmission Electron Microscopy. Nano Lett. 15(7): 4737-4744. DOI:10.1021/acs.nanolett.5b01636.

24. HUANG, B.Q.; YEUNG, E.C. Chemical and physical fixation of cells and tissues: an overview. Plant Microtechniques and Protocols, part I. Springer, 2015. pp.23-43. DOI: 10.1007/978-3-319-19944-3_2.

25. JAHN, K.; BARTON, D.; BRAET F. (2007) Correlative fluorescence- and scanning, transmission electron microscopy for biomolecular investigation. Modern research and educational topics in microscopy, vol. 1: 203-211.

26. BERTAZZO, S.; von ERLACH, T.; GOLDONI, S.; ÇANDARLIOĞLU, P.L.; STEVENS, M.M. (2012) Correlative light-ion microscopy for biological applications. Nanoscale, 4: 2851-2854. DOI: 10.1039/c2nr30431g.

27. MAYER, J.; GIANNUZZI, L.A.; KAMINO, T.; MICHAEL, J. (2007) TEM sample preparation and FIB-induced damage. MRS Bull., 32: 400-407. DOI: https://doi.org/10.1557/mrs2007.63.

28. GIANUZZI, L.A.; STEVIE, F.A. (2005) Introduction to Focused Ion Beams: instrumentation, theory, techniques, and practice. New York: Springer. pp.357. DOI: 10.1007/b101190.

29. ОЛЕЙНИКОВ, В.А.; СУХАНОВА, А.В.; НАБИЕВ, И.Р. (2007) Флуресцентные полупроводниковые нанокристаллы в биологии и медицине. Российские нанотехнологии, 2 (1-2): 160-173.
30. LEATHERDALE, C.A.; WOO, W.K.; MIKULEC, F.V.; BAWENDI, M.G. (2002) On the absorption cross section of CdSe nanocrystal quantum dots. J. Phys. Chem. B., 106: 7619–7622. DOI: 10.1021/jp025698c.
31. ZHONG, X.; FENG, Y.; KNOLL, W.; HAN, M. (2003) Alloyed Zn(x)Cd(1-x)S nanocrystals with highly narrow luminescence spectral width. J. Am. Chem. Soc., 125(44): 13559–13563. DOI: 10.1021/ja036683a.
32. HOHNG, S.; HA, T. (2005) Single-molecule quantum-dot fluorescence resonance energy transfer. Chemphyschem., 6: 956–960. DOI: 10.1002/cphc.200400557.
33. WATANABE, S.; PUNGE, A.; HOLLOPETER, G.; WILLIG, K.I.; HOBSON, R.J.; DAVIS, M.W.; HELL, S.W.; JORGENSEN, E.M. (2011) Protein localization in electron micrographs using fluorescence nanoscopy. Nat. Methods, 8 (1): 80–84. DOI: 10.1038/nmeth.1537.
34. MILLS, C.E. [online] Bioluminescence of Aequorea, a hydromedusa. [cit. 11.12.2017]. Available on WWW: <https://faculty.washington.edu/cemills/Aequorea.html>.
35. CAMPBELL, T.N., CHOY F.Y.M. (2001) The effect of pH on Green Fluorescent Protein: a Brief Review. Molecular Biology Today 2(1): 1-4.
36. PÉDELACQ, J.-D.; CABANTOUS, S.; TRAN, T.; TERWILLIGER, T. C.; WALDO, G. S. (2006) Engineering and characterization of a superfolder green fluorescent protein. Nature Biotechnology, 24: 79-88. DOI: 10.1038/nbt1172.
37. DAI, M.; FISHER, H. E.; TEMIROV, J.; KISS, C.; PHIPPS, M. E.; PAVLIK, P.; WERNER, J. H.; BRADBURY, A. R. (2007) The creation of a novel fluorescent protein by guided consensus engineering. Protein Engineering, Design and Selection, 20: 69-79. DOI: 10.1093/protein/gzl056.
38. Merck Millipore, a part of Merck [online]. 345789, FluorSave™ Reagent [cit. 11.12.2017]. Available on WWW: < http://www.merckmillipore.com/CZ/cs/product/FluorSave%E2%84%A2-Reagent,EMD_BIO-345789#anchor_PDS>.

39. Thermo Fisher Scientific [online]. ProLong® Gold Antifade Mountant cit. [11.12.2017]. Available on WWW: < https://www.thermofisher.com/order/catalog/product/P36934?ICID=search-product>.
40. Electron Microscopy Sciences [online]. Permount Mounting Medium. Technical Data Sheets. cit. 11.12.2017]. Available on WWW: < https://www.emsdiasum.com/microscopy/technical/datasheet/17986.aspx>.
41. HELL, S.W. (2009) Microscopy and its focal switch. Nature Methods, 6: 24 – 32. DOI:10.1038/nmeth.1291.
42. GIEPMANS, B.N.G. (2008) Bridging fluorescence microscopy and electron microscopy. Histochem Cell Biol., 130: 211–217. DOI: 10.1007/s00418-008-0460-5.
43. ROBINSON, J.M.; TAKIZAWA, T.; POMBO, A.; COOK, P.R. (2001) Correlative fluorescence and electron microscopy on ultrathin cryosections: bridging the resolution gap. Journal of Histochemistry and Cytochemistry, 49: 803- 808. DOI: 10.1177/002215540104900701.
44. BRAET, F.; WISSE, E.; BOMANS, P.; FREDERIK, P.; GEERTS, W.; KOSTER, A.; SOON, L.; RINGER, S. (2007) Contribution of High-Resolution Correlative Imaging Techniques in the Study of the Liver Sieve in Three-Dimensions. Microscopy Research and Technique, 70: 230-242. DOI: 10.1002/jemt.20408.
45. ALBRECHT, R.M.; GOODMAN, S.L.; SIMMONS, S.R. (1989) Distribution and movement of membrane-associated platelet glycoproteins: Use of colloidal gold with correlative video-enhanced light microscopy, low-voltage high-resolution scanning electron microscopy, and high-voltage transmission electron microscopy. American Journal of Anatomy, 185: 149-164. DOI: 10.1002/aja.1001850208.
46. GRABENBAUER, M.; GEERTS, W.J.; FERNADEZ-RODRIGUEZ, J.; HOENGER, A.; KOSTER, A.J.; NILSSON, T. (2005) Correlative microscopy and electron tomography of GFP through photooxidation. Nature Methods, 14: 857-862. DOI: 10.1038/nmeth806.
47. TSIEN, R. Y. (1998) The green fluorescent protein. Annu. Rev. Biochem., 67: 509–544. DOI: 10.1146/annurev.biochem.67.1.509.

48. NEWMAN, G.R.; HOBOT, J.A. resin microscopy and on-section immunocytochemistry. Springer Lab Manuals, 2001. pp.273. DOI: 10.1007/978-3-642-56930-2.
49. RESCH-GENGER, U.; GRABOLLE, M.; CAVALIERE-JARICOT, S.; NITSCHKE, R.; NANN, T. (2008) Quantum dots versus organic dyes as fluorescent labels. Nat Methods, 5(9):763-775. DOI: 10.1038/nmeth.1248.
50. WARD WW. (1998) Biochemical and physical properties of green fluorescent protein. In: Chalfie M, Kain S. (eds), Green Fluorescent Protein. Wiley-Liss, New York, pp. 45-75.
51. Electron Microscopy Sciences [online]. Hydroxypropyl methacrylate (HPMA) kit. EMS #14220 [cit. 13.10.2017]. Available on WWW: <https://www.emsdiasum.com/microscopy/technical/datasheet/14220.aspx>.
52. abcam [online]. Glycol methanlacrylate acrylic resin (GMA) embedding for immunohistochemistry [cit. 12.12.2017]. Available on WWW:<http://www.abcam.com/ps/pdf/protocols/gma.pdf>.
53. Electron Microscopy Sciences [online]. PEG - GMA embedding medium. EMS #14250 [cit. 12.12.2017]. Available on WWW:<https://www.emsdiasum.com/microscopy/technical/datasheet/14250.aspx>.
54. Polysciences, Inc. [online]. Nanoplast embedding kit [cit. 12.12.2017]. Available on WWW:<http://www.polysciences.com/skin/frontend/default/polysciences/pdf/361.pdf>
55. Electron Microscopy Sciences [online]. Lowicryl K4M. EMS # 14330 [cit.04.12.2017]. Available on WWW:<https://www.emsdiasum.com/microscopy/technical/datasheet/14330b.aasp>.
56. Electron Microscopy Sciences [online]. EMbed 812 kit. EMS #14120 [cit. 12.12.2017]. Available on WWW:< https://www.emsdiasum.com/microscopy/technical/datasheet/14120.aspx>.
57. REID, N. Ultramicrotomy. Practical Methods in Electron Microscopy Series: Vol. 3, Pt. 2. Amsterdam: North-Holland publishing company, 1975. 353 p.

58. PEACHEY, L. D. (1958). Thin Sections : I. A study of section thickness and physical distortion produced during microtomy. The Journal of Biophysical and Biochemical Cytology, 4(3): 233–242.
59. STEINBRECHT, R.A.; MÜLLER, M. Freeze-substitution and freeze-drying. Cryotechniques in biological electron microscopy, Part II. Berlin: Springer Berlin Heidelberg, 1987. pp 149-172. DOI: 10.1007/978-3-642-72815-0_7.
60. 17238 Sigma-Aldrich [online]. HPMA embedding kit [cit. 04.12.2017]. Available on WWW:<http://www.sigmaaldrich.com/catalog/product/sial/17238?lang=en&reregi=CZ&cm_sp=Insite-_-prodRecCold_xviews-_-prodRecCold10-1>.
61. Electron Microscopy Sciences [online]. LR White embedding medium. EMS catalog LR White medium grade #14380 and #14382 [cit. 12.12.2017]. Available on WWW:< https://www.emsdiasum.com/microscopy/technical/datasheet/14380_LR_white.aspx>.
62. Order D05. (2016) Laboratory of Morphology and Rheology of Polymer Materials, Otto Wichterle Centre of Polymer Materials and Technologies. Innovation center of the Institute of Macromolecular Chemistry, Academy of Sciences of the Czech Republic, Prague.
63. PEDDIE, C.J., BLIGHT, K., WILSON, E., MELIA, C., MARRISON, J., CARZANIGA, R., DOMART, M.C., O'TOOLE, P., LARIJANI, B., COLLINSON, L.M. (2014) Correlative and integrated light and electron microscopy of in-resin GFP fluorescence, used to localise diacylglycerol in mammalian cells. Ultramicroscopy. Aug; 143: 3-14. DOI:10.1016/j.ultramic.2014.02.001.
64. GANG, Y., ZHOU, H., JIA, Y., et al. (2017) Embedding and Chemical Reactivation of Green Fluorescent Protein in the Whole Mouse Brain for Optical Micro-Imaging. Frontiers in Neuroscience; 11: 121. DOI:10.3389/fnins.2017.00121.
65. JOHNSON, E., SEIRADAKE, E., JONES, E.Y., DAVIS, I., GRÜNEWALD, K., KAUFMANN, R. (2015) Correlative in-resin super-resolution and electron microscopy using standard fluorescent proteins. Scientific Reports 5, 9583. DOI:10.1038/SREP09583.

66. SUN, M. et al. A review of correlative light and electron microscopy (CLEM) methods, markers, and instrument set ups to study infectious disease. EC Microbiology 4.5 (2016): 787-800.

67. YANG, Z., HU, B., ZHANG, Y., LUO, Q., GONG, H. (2013) Development of a Plastic Embedding Method for Large-Volume and Fluorescent-Protein-Expressing Tissues. PLOS ONE 8(4): e60877. https://doi.org/10.1371/journal.pone.0060877.

68. WATANABE, S., JORGENSEN, E.M. (2012) Visualizing proteins in electron micrographs at nanometer resolution. Methods Cell Biol.; 111:283-306. DOI:10.1016/B978-0-12-416026-2.00015-7.

69. BELL, K., MITCHELL, S., PAULTRE, D., POSCH, M., OPARKA, K. (2013) Correlative Imaging of Fluorescent Proteins in Resin-Embedded Plant Material1. Plant Physiology; 161(4):1595-1603. doi:10.1104/pp.112.212365.

70. RULLGÅRD, H., ÖFVERSTEDT, L.-G., MASICH, S., DANEHOLT, B. and ÖKTEM, O. (2011) Simulation of transmission electron microscope images of biological specimens. Journal of Microscopy, 243: 234–256. DOI:10.1111/j.1365-2818.2011.03497.x.

71. GAO, X., NIE, S. (2003) Molecular profiling of single cells and tissue specimens with quantum dots. Trends Biotechnol. Sep; 21(9):371-373. DOI: 10.1016/S0167-7799(03)00209-9.

72. McDONALD, K.L, WEBB, R.I. (2011) Freeze substitution in 3 hours or less. J Microsc. Sep; 243(3): 227-33. DOI: 10.1111/j.1365-2818.2011.03526.x.

APPENDIX 1. Table 1. Resin methodology for localization of cellular structures with EM (based on Ref.48)

APPENDIX 2. Table 2. Characteristics of fixative agents used in LM and EM (based on Ref.24)

Fixative agent		**Properties**	**Impact on biological componets**	**Result**
1		***2***	***3***	***4***
Coagulant	Ethanol	Dehydrating solvent for LM and EM. (Farmer's fixative (ethanol:acetic acid; 3:1, v:v) preffered for laser-capture microdissection methods.	Unfixed proteins are coagulated by ethanol. Precipitate proteins by replacing water.	Good preservation of nuclear morphology. Conformation and solubility change of protein molecules. Lipids are not preserved. Shrinkage effect.
	Methanol			Good preservation of nuclear morphology. Conformation and solubility change of protein molecules. Lipids are not preserved.
	Acetone	Cold acetone fixation maintain enzyme activity. Miscible with epoxy resins.	Dehydration of tissues. Precipitate proteins by replacing water.	Conformation and solubility change of protein molecules. Make the tissue more brittle.
Non-coagulant	Acetic acid	Does not react with proteins. Fast penetration. Farmer's fixative (ethanol:acetic acid; 3:1, v:v) preffered for laser-capture microdissection methods. Formalin–acetic acid–alcohol (FAA) is the most common	Coagulation of nuclear proteins. Prevent the loss of nucleic acids.	Swelling of cells. In conjunction with ethanol gives suppression of shrinkage effect.

1	2	3	4
	botanical fixative for the paraffin-embedded method.		
Formaldehyde	Quick penetration due its molecular weight. Longer fixation time. Toxic one. To prevent self-polymerization methanol is added as a stabilizer. Recommends to use only fresh made solution and use it immideately. Could be combined with glutaraldehyde.	Slow forming of stable methylene bridges with protein nitrogen. Intra- and intermolecular cross-links.	Better preservation of the cellular organization.
Glutaraldehyde	For ultrastructural studies. Slow penetration. Could be combined with formaldehyde. Not compatible with paraffin-embedding medium.	Irreversible reactions with macromolecules. Inhibits enzyme activity. Intra- and intermolecular cross-links.	Fixed specimes have a high level of fluorescence. Better preservation of the cellular organization.
Osmium tetroxide (OsO_4)	Slow penetration (0.25 mm/h). Sublimate into vapor from a solid state, could cause blindness. Mainly used as a secondary fixing agent.	Reacts with unsaturated lipids. Intra- and intermolecular cross-links.	Glycol methacrylate is not compatible with it.

1		*2*	*3*	*4*
	Glyoxal	A “formalin substitute”		A pleasing effect in histology and immunohistochemistry
	Carbodiimides		Effective as tissue fixative	For immunohistochemical studies.

APPENDIX 3. Table 3. Comparison of properties of QDs and organic dyes.[49]

Property	Quantum dot (dependent on material, size, size distribution and surface chemistry)	Organic dye (dependent on dye class and are tunable via substitution pattern)
1	*2*	*3*
Absorption spectra	Steady increase toward UV wavelengths starting from absorption onset; enables free selection of excitation wavelength	Discrete bands, FWHM of the maximum 35 nm (fluoresceins, rhodamines and cyanines) to 80-100 nm (CT dyes, such as coumarins, for example)
Molar absorption coefficient	10^5-10^6 $M^{-1}cm^{-1}$ at first exitonic absorption peak, increasing toward UV wavelength ; larger (longer wavelength) QDs generally have higher absorption	$2.5\times10^4 - 2.5\times10^5$ $M^{-1}cm^{-1}$ (at long-wavelength abruption maximum)
Emission spectra	Symmetric, Gaussian profile; FWHM, 30-90 nm	Asymmetric, often tailing to long-wavelength side; FWHM, 35 nm (fluorosceins, rhodamines and cyanines) to 70-100 nm (CT dyes)
Stokes shift	Typically <50 nm for visible wavelength-emitting QDs	Normally <50 nm (fluoresceins, rhodamines and cyanines), up to >150 nm (CT dyes)
Quantum yield	0.1-0.8 (visible: 400-700 nm), 0.2-0.7 (NIR: >700 nm)	0.5-1.0 (visible), 0.05-o.25 (NIR)
Fluorescence lifetimes	10-100 ns, typically multi-exponential decay	1-10 ns, mono-exponencial decay
Two-photon action cross section	2×10^{-47}-4.7×10^{-46} cm^4 s $photon^{-1}$	1×10^{-52}-5×10^{-48} cm^4 s $photon^{-1}$ (typically about 1×10^{-49} cm^4 s $photon^{-1}$
Solubility or dispersibility	Control via surface chemistry (ligands)	Control by substitution pattern
Binding to biomolecules	Via ligand chemistry; few protocols available. Several biomolecules bind to a single QD. Very little information available on labeling-induced effects	Via functional groups following established protocols. Often several dyes bind to a single biomolecule. Labeling-induced effects on spectroscopic properties of reporter studied for many common dyes.
Size	6-60 nm (hydrodynamic diameter); colloid	~0.5 nm; molecule

1	*2*	*3*
Thermal stability	High; depends on shell or ligands	Dependent on dye class; can be critical for NIR-wavelength dyes.
Photochemical stability	High (visible and NIR wavelengths); orders of magnitude higher than that of organic dyes; can reveal photobrightening	Sufficient for many applications (visible wavelength), but can be insufficient for high-light flux applications; often problematic for NIR-wavelength dyes
Toxicity	Little known yet (heavy metal leakage must be prevented, potential nanotoxicity)	From very low to high; dependent on dye
Reproducibility of labels (optical, chemical properties)	Limited by complex structure and surface chemistry; limited data available; few commercial systems available	Good, owing to defined molecular structure and established methods of characterization; available from commercial sources
Applicability to single-molecule analysis	Good; limited by blinking	Moderate; limited by photobleaching
Fluorescence Resonance Energy Transfer (FRET)	Few examples; single-donor-multiple-acceptor configurations possible; limitation of FRET efficiency due to nanometer size of QD coating	Well-described FRET pairs; mostly single-donor-single-acceptor configurations; enables optimization of reporter properties
Spectral multiplexing	Ideal for multi-color experiments; up to 5 colors demonstrated	Possible, 3 colors (MegaStokes dyes), 4 colors (energy-transfer cassetes)
Lifetime multiplexing	Lifetime descimination between QDs not yet shown; possible between QDs and organic dyes	Possible
Signal amplification	Unsuitable for many enzyme-based techniques, other techniques remain to be adapted and/or established	Established techniques

APPENDIX 4. Table 4. Observed colors and measured thicknesses of the sections by Peachey L.D. [Ref. 58, edited]

Measured thickness (μm)	Color observed at 15° to normal	Effective thickness for θ=15° (μm)
49	Gray	48
49	Gray	48
49	Gray	48
49	Gray	48
64	Grayish silver	63
64	Silver	63
83	Silver	82
85	Silver	84
88	Silver	87
92	Silver	91
95	Gold	94
110	Silver	108
125	Gold-silver	123
125	Gold	123
127	Gold	125
128	Gold	126
135	Reddish gold	133
166	Reddish gold	164
200	Purple	197
239	Sky-blue	235
264	Yellow	260
278	Yellow-green	274

APPENDIX 5.

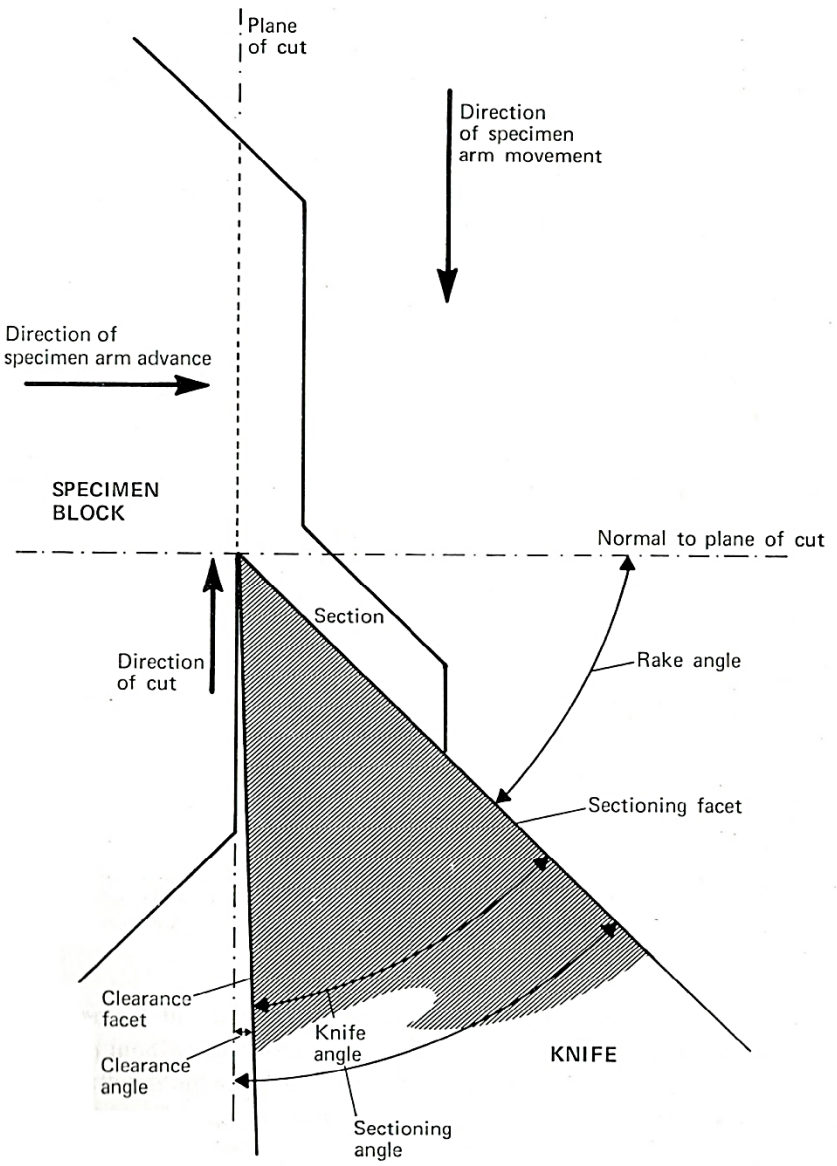

Figure. The process of section formation.[57]